Politecnico di Torino

Politecnico di Torino

Master's Degree in Civil Engineering

Academic Year 2024/25

Structural Reliability of Reinforced Concrete Frames Under Column Removal Scenarios

Supervisor:

Diego Gino

Co-supervisor:

Elena Miceli

Candidate:

Juan Jose Montoya Duque

S306628

Acknowledgement

A mi familia, por su amor incondicional, por siempre creer en mí y apoyarme en todo momento.

A mis amigos, que aun en la distancia, siempre estuvieron presentes.

A la familia que encontré en mi camino por Torino, gracias por hacer este proceso más bonito.

Abstract

Structural robustness has been a topic of particular interest, especially after two significant events: the partial collapse of the Ronan Point building in London and the attack on the World Trade Center in New York. These incidents led to an evaluation of the capacity of structures to withstand partial failures that could lead to progressive collapse. International standards, such as the Eurocode and ISO, have developed strategies to enhance structural resistance and reduce the risk of progressive collapse.

To evaluate the robustness of a building in a quantitative way, methods such as the "stiffness-based measure" and "energy-based measure" have emerged. These approaches assign a robustness value to the structure, with the goal of determining structural reliability, where probabilistic methods are commonly applied.

A practical approach to evaluate structural robustness is the Pushdown Analysis. A practical exercise consists of removing a first-story column from a building and applying an imposed displacement at the location where the column was removed, allowing for a step-by-step observation of the structural response to local damage.

The Pushdown Analysis is performed using finite element software ATENA 2D v5, evaluating a five-story building with four spans and a regular configuration in plan and elevation. Three different structures are analyzed to evaluate the resistance to progressive collapse by evaluating the structural reliability involving the removal of the second-to-last supporting column. The first structure is designed according to standard codes, while the second and third structures incorporate robustness enhancements regarding the arrangement of the longitudinal reinforcement of the beams.

Table of Contents

List of Figures

1. Introduction

Structural robustness has been of significant importance in civil engineering after unfortunate events such as the partial collapse of the Ronan Point Building in London (1968), the collapse of the Alfred P. Murrah Federal Building in Oklahoma (1995), and the attack on the World Trade Center in New York (2001). These incidents exposed the vulnerability of structures to extreme events and led to the development of strategies to mitigate the risk of progressive collapse. Various authors have defined structural robustness as the capacity of a structure to resist local failures without leading to a disproportionate collapse. This requires considering important characteristics like ductility, redundancy, and continuity within the structures.

Several international codes have established strategies to ensure structural robustness and minimize the effects of damage. The Eurocode EN 19991-1 proposes design strategies that include the identification and mitigation of accidental loads, protect the structure against extreme events, and increase the capacity of key structural elements to enhance overall resistance. On the other hand, ISO 2394 suggests a structural design approach based on the control of events, specifying adequate load resistance, providing alternative load paths and the redundancy of the structures.

For the measurement of structural robustness, various approaches have been proposed, such as the stiffness-based measure and the energy-based measure methods. Starossek y Haberland (2010) proposes strategies where stiffness-based

approach quantifies the capacity of a structure to maintain its integrity when a critical structural element is removed, while the energy-based approach compares the energy released during the initial failure with the energy required for the collapse during the initial failure with the energy required for the collapse to progress. Both methods allow the evaluation of structures' vulnerability.

On the other hand, structural reliability is a concept that evaluates the probability of structural failure under several conditions. It can be approached from a probabilistic perspective, based on the theory developed by Haldar and Mahadevan (2000), as well as through semi-probabilistic and deterministic methods. Considering the typical uncertainties in the parameters that influence the behavior of the structure, highlight the random uncertainties and epistemic uncertainties.

The pushdown analysis is a method that allows evaluating the capacity of a structure against progressive collapse. This approach is based on the pushover methodology used in seismic engineering, allowing the quantification of a building capacity after the loss of a key structural element. Authors such as Khandelwal and Tawil (2011) and Fallon et al. (2014) have proposed some variations of this analysis, such as Uniform Pushdown and Bay Pushdown, which allow collapse modes to be characterized and provide detailed information about the structural response.

In this thesis, the structural reliability of a reinforced concrete building subject to the remotion of the second-to-last column is studied. The simulations are carried out using FEM software, specifically ATENA 2D v5, which allows modeling the nonlinear response of the structure and evaluating its behavior. This work is based on the studies conducted by Miceli (2024), where the structure is designed according to

Italian code (NTC 2018) and the Eurocode. The model incorporates equivalent springs that represent the contribution of transverse elements.

The failure scenario is evaluated through three structural frames, which share the same geometry, but vary in design. The variations are related to the implementation of current robustness strategies and new proposed improvements suggested by Miceli and Castaldo (2024). These new proposed strategies include Continuity, Global floor equality and side face rebar. To evaluate the effectiveness of these improvements and structural behavior, a Pushdown analysis is performed to obtain the capacity curves of each frame. Additionally, material and load aleatory properties are considered using a Latin Hypercube Sampled method, generating 100 variations of the material properties and loads, resulting in 100 models for each frame.

Finally, the probability of structural failure can be computed following the methodology proposed by Miceli et al. (2025), this procedure consists of five steps. First, aleatory properties for materials and actions are sampled, generating 100 sets of variables. Second, a pushdown analysis is performed, where structural reaction under imposed vertical displacement is monitored. Third, the dynamic amplification factor is determined by equating the external work with the internal energy of the structure. Fourth, an equivalent static analysis is executed to examine the principal total strain at the nodes. Then, the probability of failure is computed through a convolution integration, evaluating the structural capacity with the structural demand. The results show how structural improvements enhance the response of the structure, reducing the probability of failure.

2. History and robustness definitions

2.1. History

The importance of structural robustness was increased after the partial collapse of the Ronan Point Building in London on May 16th of 1968. Figure 2.1 shows how an explosion of gas in some of the upper floors of the Ronan Point Building caused a progressive collapse of several floors. This event marked an important milestone that led to the inclusion of progressive collapse risk in construction codes and guidelines, emphasizing the necessity of continuity and redundancy in structures to avoid similar failures.

Figure 2.1 *Ronan point building after collapse (Pearson and Delatte,2005)*

However, according to Adam et al. (2018), the studies about the progressive collapse of structures began a couple of decades before, during the Second World War, when Lord Baker analyzed the behavior of the buildings damaged by bombs in London.

Lately, events like the collapse of the Alfred P. Murrah Federal Building in Oklahoma on the 19th of April of 1995 highlighted the vulnerability of structures to extreme events. This terrorist attack led to the introduction of new standards and recommendations about structural robustness.

The event that brought greater relevance to the concept of structural robustness was the terrorist attack on the World Trade Center in New York on the 11th of September of 2001, as seen in Figure 2.2. This attack caused the collapse of the Twin Towers and more buildings and had a significant impact on public awareness about the importance of safety and robustness in structures.

These tragic events highlighted the necessity to design stronger structures capable of resisting localized damage without undergoing a total collapse.

Figure 2.2 Attack on World Trade Center (Ślaga,2013)

2.2. Structural robustness definition

The structural robustness is defined by different authors and papers like:

According to Baker et al. (2008) it is defined as the capacity of a structure to resist the total or disproportional collapse when this is subject to exceptional events or local damage that were not considered in a conventional design. This implies that the consequences of a structural failure should not be disproportionate concerning the event that caused it. In this context, a robust system is not only capable of withstanding the expected loads during its service life but also standing damage or exceptional events without totally collapsing.

On the other hand, according to Adam et al. (2018), structural robustness is described as the insensitivity of a structure to local damage. In other words, a robust structure is one that can withstand damage in a specific area without leading to a general collapse.

In conclusion, as mentioned by Agarwal and England (2008), structural robustness can be understood as the capacity of a structure to withstand unexpected events or damage, such as explosions, impacts, human errors, or material degradation, without disproportionate consequences in relation to the initial damage. This means a robust structure can suffer unexpected events without collapse disproportionately to the initial damage.

According to Fascetti et al. (2015), It is important to highlight the term progressive collapse, which is usually the result of a chain reaction that begins with local damage in one or more structural elements caused by overload or extraordinary load. The origin and magnitude of the loads can vary in any case, when the local capacity of a key element is reached, the failure of a large portion or the whole structure can occur.

It can be said that the building with structural robustness has characteristics such as:

- *Ductility*, which is the capacity of materials to deform without breaking, absorbing energy and distributing the loads during an extreme event.

- *Redundancy*, which refers to the presence of multiple load paths that can assume the load if an element fails, which allows the structure to carry loads even in the event of the failure of one element.
- *Continuity*, the continuity between structures is represented by the continuity of the longitudinal reinforcement through support. This is essential to ensure the redistribution of loads in the event of an element failure.

3. International design codes about robustness

Different international codes discuss strategies that should be taken into account to prevent progressive collapse and ensure the robustness of a structure.

3.1 Strategies according to Eurocode

Specifically, Eurocode EN 1991-1-7, Annex A provides various strategies to consider for accidental design situations, which are illustrated in Figure 3.1 below.

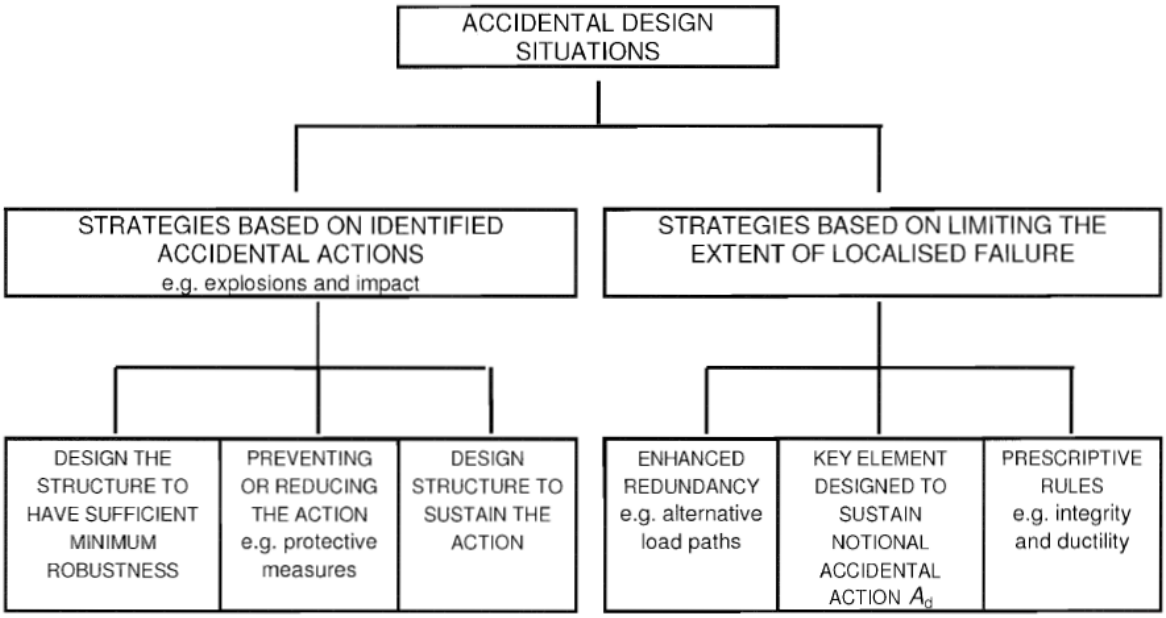

Figure 3.1 *Accidental design situations (EN1991-1-7 Annex A)*

These situations are strategies for identifying accidental actions and strategies to limit the extent of localized failure.

In the first place, the strategies aimed at mitigating the risk of identified accidental loads are the following:

- Preventing or reducing the probability or magnitude of the event (e.g. providing adequate clearances between traffic lanes and the structure in bridges).
- Protecting the structure from the effects of accidental events (e.g. using protective bollards or safety barriers).
- Ensuring the robustness of the structure through the adoption of the following approaches:
  i. Designing of key elements to improve the probability of the structure surviving accidental events.
  ii. Select materials and design structural members with sufficient ductility to absorb significant strain energy without fail.
  iii. Incorporate sufficient structural redundancy to enable load transfer to alternative paths in the event of a failure.

On the other hand, to limit the extension of localized structural failure, one or more of the following approaches should be implemented:

- Design of key elements to sustain the effects of accidental actions.
- Design the structure to avoid localized failures that affect the global stability of the structure.

- Applying prescriptive design and detailed rules to guarantee the robustness of the structure.

According to EN 1990 – Basis of Structural Design, for each critical load situation, the design effects (E_d) must be determined by combining the actions that occur at the same time. In the case of an accidental design situation, the combination of actions is the following:

$$\sum_{j>1} G_{k,j} \text{"+"} P \text{ "} + \text{"} A_d \text{"} + \text{"} \Psi_{2,1} Q_{k,1} \text{"} + \text{"} \sum_{j>1} G_{k,j}\, Q_{k,i}$$

The choice of variable parameters should be related to the specific accidental design situation, considering both favorable and unfavorable cases. The "+" symbol indicates combinations, where P represents the prestressing load and A_d is the design value of the accidental load.

3.2 Strategies according to ISO 2394

The standard code ISO 2394, in Annex F, discusses structural robustness and provides appropriate design strategies, which can be classified as follows:

- *Event control*: This is an indirect method aimed at reducing the probability of accidental events. This means protecting against incidents that could lead to significant failures in a structure. However, this method does not make the structure stronger against such failures. The effectiveness of this approach depends on whether users follow the designer's rules and recommendations.

- *Specific load resistance*: This is a direct method that reduces the probability of local damage due to an accidental event. It ensures that certain parts of a structure, known as key elements, are strong enough to resist damage from accidental loads. Key elements examples include columns, load-bearing walls, bridge piers, or cables in suspension structures. If these elements fail, it can cause further damage since the structure will not have alternative load paths to carry the loads.

- *Alternative load paths*: This approach is a direct method that aims to reduce the probability of further damage in the case of local damage. This method analyzes alternative paths for transferring loads from the point of application to the point of assessment. This method examines what happens when structural members are removed sequentially, allowing forces to be redistributed along new alternative paths to observe if they are strong enough to prevent failure from spreading.

- *Reduction of Consequences*: This is an indirect method that reduces the consequences of follow-up damage, such as progressive collapse. The goal is to reduce the impact of failure and the risk. Measures in this category can include structural and architectural changes, such as the provision of escape routes. The objective is to enhance safety through effective planning and the use of equipment.

4. Measure of structural robustness

Previously, the definition of structural robustness was discussed, with several approaches to enhance and ensure it, all evaluated from a qualitative perspective, ensuring the response to progressive collapse.

Now, from a quantitative approach to evaluate robustness, Starossek and Haberland (2011) suggest that a structure should be quantified with a unique valor that reflects the impact of abnormal events on design objectives, thus improving the management of robustness in the design and evaluating of structures, their application includes:

Optimization, which facilitates the improvement of structural design. *Regulation*, which allows the definition of minimum robust requirements in standards and guidelines. *Evaluation*, which helps to identify critical elements and compare different designs. *Design assistance*, which supports the decision whether additional measures against progressive collapse are required. *Safety factors*, where a factor could be included to consider the response of initial structural failure.

However, the validity and use of robustness and collapse resistance measures depend on several general requirements such as:

- *Expressiveness*: The measure must clearly reflect the robustness of the structure, distinguishing between safety and vulnerable structures.
- *Objectivity*: The measure must be independent of the user, with reproducible values in similar conditions.
- *Simplicity*: The definition must be simple to facilitate use and acceptance.

- *Calculability*: It should be derivable from the structure properties, with accurate and not excessively complex calculations.
- *Generality*: The measure should be applied to any type of structure.

In the studies conducted by Starossek and Haberland (2011), there were proposed different quantitative approaches to measure structural robustness, which are:

4.1. Stiffness-based measure of robustness

This measurement of robustness is derived by examining the static stiffness of the system. A simple way to calculate it is by using the following formula:

$$R_s = min_j \frac{\det K_j}{\det K_0}$$

Where R_s is the robust measure based on stiffness, K_0 is the stiffness matrix of the active system of the intact structure, K_j is the stiffness matrix of the active system of the structure after removing a structural element or connection j.

To obtain a practical measure with a range between 0 and 1, this expression must be calibrated. A value of 1 represents the maximum possible robustness, while a value of 0 means a total lack of robustness. The intermediate values have the purpose of providing quantitative and expressive measures of robustness.

The advantages of simplicity and ease of calculation make the assessment of robustness using a system of matrices a valuable tool. However, this

measure of robustness based on stiffness reflects more the connectivity of the system than the actual structural robustness. This is because the reduction in load-carry capacity by removing a structural element does not always directly correlate with the values of R_s.

Despite this limitation, the simplicity of the calculation of this measure justifies its use in structural robustness assessment. In addition to stiffness, other structural properties such as strength, load-bearing capacity, ductility, and mass distribution can also be described using the corresponding matrices systems and be included in such evaluation.

4.2. Energy-based measure of robustness

The following formula for measuring of structural robustness based on energy compares the energy released during an initial failure with the energy needed for the failure to progress.

$$R_e = 1 - max_j \frac{E_{r,j}}{E_{f,k}}$$

Where, R_e is the measure of robustness based on energy, $E_{r,j}$ is the energy released during the initial failure of a structural element j that contributes to damaging a subsequently affected structural element k, and $E_{f,k}$ is the energy required for the failure of the subsequently affected structural element k.

This simple formula allows us to check if a structure can withstand a total collapse. A value of 1 indicates perfect robustness, values between 0 and 1

are acceptable, and negative values indicate a progressive collapse. A challenge is accurately calculating the energy released during the initial failure of the element, especially in structures vulnerable to domino-type collapse, where the potential energy is converted into kinematic energy. In other types of collapse, a more detailed analysis is required. Furthermore, the parameter $E_{r,j}$ should only include the energy that generates damage to element k, making it more useful for structure vulnerable to domino-type collapse. It is particularly relevant when the failure of k leads to total collapse and elements j and k are similar and are completely composed of these elements.

5. Structural reliability

The occurrence of several outcomes for a determinant phenomenon is identified with the term uncertainty or randomness, in every engineering analysis, there is part of uncertainty and variation in the results, even when performing the exact same analysis. This is why it is extremely important to conduct a significant number of tests and carry out probabilistic analysis to achieve a reliable result.

5.1. Basic of probability

According to Haldar and Mahadevan (200), Probability is based on identifying all the possible outcomes of a problem, it means its uncertainty, which is mathematically described by the set theory. This theory says that a sample space includes all possible sample points, which can be mutually exclusive. The events are subsets of the sample space and can be combined using union, intersection, and complement rules. Furthermore, the events can be *impossible* when they have no sample points, *certain*, when they contain all sample points, and each event also has its complements, this means, the opposite of what it describes.

Haldar and Mahadevan (2000), in their book, discuss some basic terms of probability, like the three fundamental axioms of probability, which are:

1. The probability of an event is always nonnegative $P(E) \geq 0$.

2. The probability of the sample space $(S)$is 1 $P(S) = 1$.

3. If two events are mutually exclusive, the probability of their union is equal to sum of their probabilities:

$$P(E_1 \cup E_2) = P(E_1) + P(E_2)$$

This means that whenever we have an event E, its complement is calculated as:

$$P(E_c) = 1 - P(E)$$

The *Multiplication Rule* is used to calculate the probability of the intersection of events, which depends on their statical independence. If the events are independent, the probability of both occurring is the product of their individual probabilities.

$$P(E_1 \cap E_2) = P(E_1)P(E_2)$$

Additionally, if the events are mutually exclusive, the probability of their intersections is zero.

The total probability theorem allows us to determine the probability of an event that can be caused by different possibilities. This theorem says that the probability of an event X occur is the sum of all the possibilities that it can happen, weighted by the probability of each cause.

$$P(X) = \sum P(X|Ei)P(Ei)$$

On the other hand, Bayes' theorem allows us to find the probability of an event E_i given that event A has already occurred, this can be calculated using the total probability theorem, making it an inverse problem.

$$P(E_i|A) = \frac{P(A|E_i)P(E_i)}{P(A)}$$

5.2. Uncertainty

In the context of structural safety assessment in reinforced concrete structures, Miceli et al. (2024) talks about uncertainty as the lack of certainty in the knowledge of the parameters that influence a structure's behavior. These uncertainties can affect the prediction of structural strength and safety, furthermore, these can arise from diverse sources.

Additionally, they are classified into two main categories: random uncertainties and epistemic uncertainties.

- *Random uncertainties* represent the inherent variability in material properties and geometry of structural elements. In the case of material, this includes variations in properties such steel yielding strength (F_y), compressive strength (F_c) and modulus of elasticity (E_s), these properties are generally modeled using probabilistic distributions, like as the lognormal distribution. In the case of geometry, it includes variations in elements dimensions (thickness, width, height.) and the load eccentricities, these variations are typically characterized by normal distributions.

- *Epistemic uncertainties* are related to the limitations of numerical models used to evaluate structural resistance. This is due to the necessary simplifications in the modeling of structural behavior, including assumptions about the constitutive laws of materials and kinematic compatibility. Epistemic uncertainties are typically represented using lognormal probabilistic distributions.

5.3. Concept of reliability

The concept of structural reliability is based on the idea of determining the probability of structural failure, ensuring structural safety and performance under several conditions. Structural reliability can be estimated using different approaches, Miceli (2024) mentions some of these approaches.

- *Deterministic approach*, this method uses nominal values of basics variables and an empirical safety factor to determine the structural reliability, its formula is:

$$R_{nom} \geq \gamma \, E_{nom}$$

Where R_{nom} is the nominal resistance, E_{nom} is the nominal demand and γ is a global safety factor. Nowadays, probabilistic approaches are preferred, making this method largely obsolete.

- *Semi-probabilistic approach*, this method simplifies the probabilistic distribution of basic variables by using design values, and if the following conditions are satisfied, the structure is considered safe:

$$g(X) = R_d - S_d > 0$$

Where R_d represents the design resistance, S_d represents the design action effect and X is a vector of design parameters. Moreover, it can be said that the design values are obtained from characteristic values of materials and loads, adjusted by partial safety factors. As a particularity, the Eurocode uses this method to evaluate structural reliability.

- *Probabilistic approach*, this is based on advanced probabilistic techniques, particularly first-order reliability methods, which include various approaches, such as the first order second-moment methos (FOSM).

In this method, the limit state function ($Z = R - S$) is linearized using a first-order Taylor series expansion and considering only the second-order moments (means and covariances) of the random variables.

The reliability index is found using the means and standard deviations of R (resistances) and S (load), where both are defined as normally distributed and statistically independent random variables.

$$\beta = \frac{\mu_R - \mu_S}{\sqrt{s_R^2 - s_S^2}}$$

6. Methods to evaluate progressive collapse

Continuing with the assessment of structural robustness, it is essential to implement a technique that allows the simulation of the loss of a critical structural element, like a column, in order to analyze the structure capacity to maintain its functionality under such scenario. A valuable method is pushdown analysis, which allows the quantification of structural robustness against progressive collapse.

6.1. Pushdown analysis

The pushdown analysis is an analytical technique inspired by the pushover analysis, which is used in seismic engineering. This method simulates how a damaged structure supports increasing gravitational loads until it reaches a failure state, defined as the system's incapacity to support the applied loads.

According to Fallon et al. (2016), pushdown analysis simulates how a structure response to local damage, determining its residual capacity and providing a more detailed evaluation that the current “pass/fail methods”, which do not take into account potential failure modes, or the degree of robustness provided by structural reinforcement. It can be considered like the pushover Method, both methods increase the load progressively until the structure reaches a failure point, offering a more detailed view of its behavior under extreme conditions.

The Overload Factor (OF), according to Khandelwal and Tawil (2011), is defined as the ratio between the failure load (the maximum load that the structure can withstand before collapsing) and the nominal gravitational load applied to the system. In other words, the overload factor quantifies how many times the structure can support the nominal load before it failure, this is expressed with the following formula:

$$Overload\ Factor(OF) = \frac{Failure\ load}{Nominal\ gravity\ load}$$

Additionally, some variations of pushdown analysis are mentioned by Khandelwal and Tawil (2011) and Fallon et al. (2014), such as Uniform pushdown (UP) and Bay pushdown (BP).

- *Uniform Pushdown (UP)*, this method consists of uniformly increasing the gravitational loads on the damaged structure until collapse occurs. This failure typically occurs in the weakest area of the structure. However, this approach should not accurately capture the local response in the damaged regions. To obtain more reliable results, it is recommended to apply this method to complete 3D models, as they allow considering the load redistribution and the identification of potential failures in different parts of the structure. On the other hand, 2D analyses provide a more limited and less representative view of the global structure response.

- *Bay Pushdown (BP)*, in this approach, the gravitational load increases only in the damaged areas, while the rest of the structure maintains nominal loads.

This allows the evaluation of residual capacity and finding collapse modes that initiate locally in the affected zones.

The bay pushdown method allows the identification of two modes in which collapse can occur. The first one is called *Contained Collapse Mode (CCM)*, which occurs when the failure is limited only to the damaged areas, and the second one, known as *Propagated Collapse Mode (PCM)*, occurs when the failure spreads to adjacent areas, compromising more broadly the integrity of the structure.

In the interpretation of pushdown analysis results carried out by Khandelwal and Tawil (2011), it is important to highlight the *Catenary effect*, which is developed when beams resist vertical loads through a cable-like mechanism. To activate this mechanism, the beam-column connection must be sufficiently ductile, and there must be sufficient anchorage capacity at the end of the members. In structures with weak connections, catenary action is not fully reached due to column buckling, in contrast, in structures with stronger connections, catenary action plays an important purpose in collapse resistance.

7. Reinforced concrete building and FEM modelling

Based on the studies conducted by Miceli (2024), this thesis analyzes the structural robustness of one of the proposed models. Specifically, it focuses on the second failure scenario presented by Miceli and Castaldo (2023). In this scenario, the second-to-last column B is removed, as shown in the following Figure 7.1.

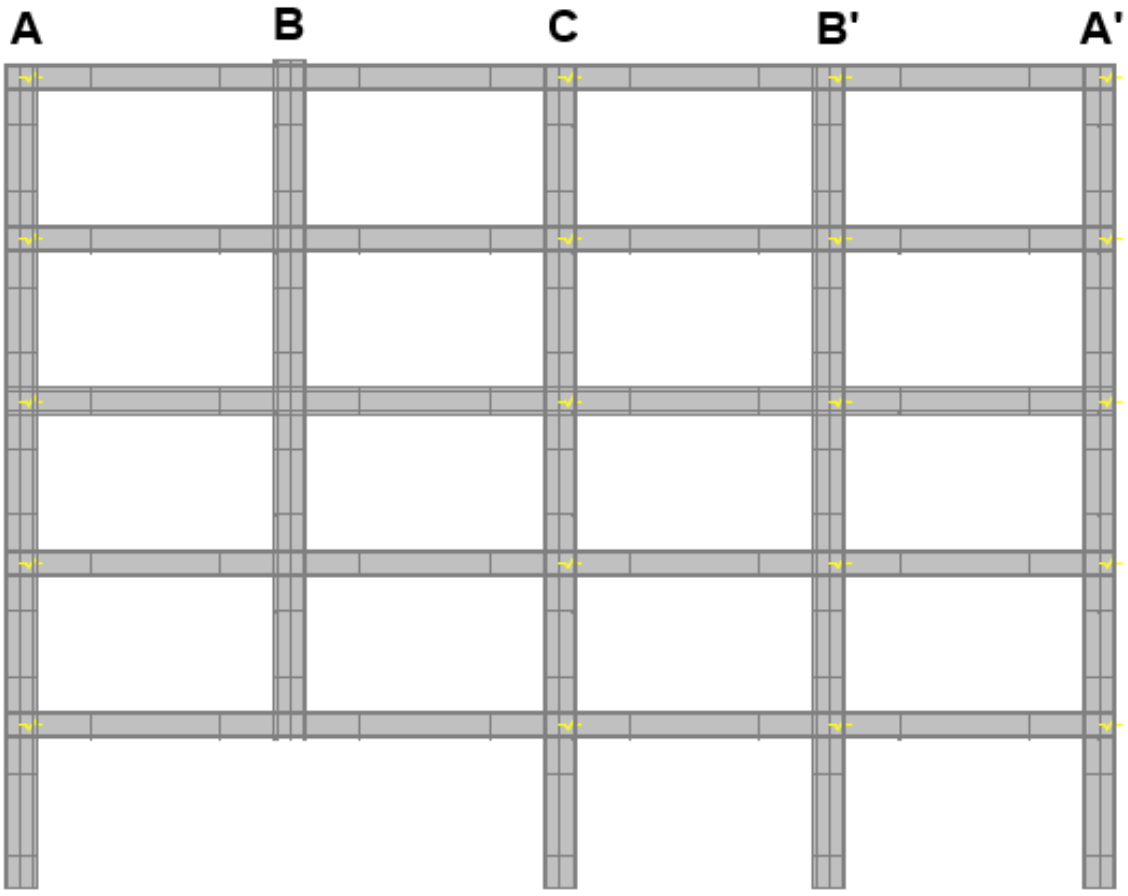

Figure 7.1 *Scenario of study*

7.1. Description of multistory RC building

Before mentioning the size dimension and reinforcement design of the building, it is important to establish some assumptions. The building is located in a high-seismicity area, such as L'Aquila in Italy, a place widely studied due to the earthquake that occurred in 2009. It is designed according to the Italian code (NTC 2018) and Eurocode 8 - Design of Structures for earthquake resistance. Additionally, the building is considered a high-ductility class structure, or CD "A" as stated in the NTC 2018.

Regarding the seismic action, Miceli (2024) adopted the following assumptions:

- Design reference period V_N= 50 years
- Ground type: B (according to NTC 2018" *Soft rocks and deposits of highly compacted coarse-grained soils or very consistent fine-grained soils, characterized by an improvement in mechanical properties with depth and by equivalent velocity values between 360 m/s and 800 m/s.")*
- Topography class: T3 (according to NTC 2018 "Reliefs with a crest width much smaller than at the base and an average inclination of 15° to 30°.")
- Damping factor of 5 %
- Behavior factor q=5.85. DC "A", αu/α1=1.3 for multi-story multi-bay frames and $K_w = 1$ for frame systems.

- Peak ground acceleration Ag=0.104g at the operational limit state and 0.261g at the Life safety limit state.

The building is described as a 5-story structure, with an inter-story height of 3 m, except for the first floor, which has a height of 3.25 m. It has 4 spans of 5 m each. Second to last Column B is removed, as is shown in figure 7.1.

The RC building is classified as regular both in elevation and in plan. Additionally, it is classified in exposure class XC2 (which, according to UNI EN 206-1, is wet, rarely dry, it refers to environments where concrete structures are exposed to moderate humidity, such as buried structures).

According to Eurocode 1 the following loads are considered: permanent structural loads (G1), Non-structural permanent loads (G2), Variable loads (Q), which included live loads (Q1), wind load (Q2) and snow load (Q3), additionally is considered the seismic action (E). The respective load values are taken from Miceli (2024) and are shown in Table 7.1.

With all the previously mentioned considerations. Regarding ultimate limit state (USL) and serviceability limit state (SLS), Miceli and Castaldo (2024) compute the design of the building, which has the following details.

Size dimensions

- Beam cross section: $40x50\ cm^2$
- Column cross section: $60x60\ cm^2$

(Since this thesis considers a 2D study case, in the model, the column section is 60 cm, and the beam section is 50 cm.)

Table 7.1 *Summary actions (Miceli, 2024)*

Action	***Type of action***	***Values***	
Permanent structural load (G_1) (mean value)	Beam and column self-weight.	Assuming a specific weight of 25 kN/m^2	
	Slab self-weight.	3.2 kN/m^2	
Permanent non-structural load (G_2) (mean value)	Screed, pavement and plaster.	1.4 kN/m^2	
	Internal partition.	1.2 kN/m^2	
Live load (Q_1) (characteristic value)	Floors.	2 kN/m^2	
	Roof.	0.5 kN/m^2	
Snow (Q_2) (characteristic value)	Roof.	2.17 kN/m^2	
Wind (Q_3) (characteristic value)	Height	Upwind	Downwind
	3 m	0.72 kN/m^2	-0.36 kN/m^2
	9 m	0.72 kN/m^2	-0.36 kN/m^2
	15 m	0.79 kN/m^2	-0.36 kN/m^2

Regarding the concrete, a compression strength class C25/30 was proposed, with 3.5 cm of concrete cover for all elements. Furthermore, the steel reinforcement bars used are B450C. The building's steel arrangement is described below.

- *Beam arrangement*: Longitudinal steel reinforcement consists of ϕ18 bars, while the transverse reinforcement is made of 2-legs ϕ8 bars with a spacing of 10 cm in the dissipative zone (D), which has a length of 1 m, and 15 cm in the non-dissipative zone (ND).

- *Columns arrangement*: longitudinal steel reinforcement is composed of 12ϕ20 bars, symmetrically arrangement in both directions, while the transverse reinforcement is made of 4-legs ϕ8 bars, with a spacing of 10 cm along the entire column height.

- Beam-column arrangement: The transverse steel reinforcement consists of 4-legs ϕ8 bars with a spacing of 5 cm.

Table 7.2 below has a summary of reinforcement detailing the building for floors.

Table 7.2 *Reinforcement arrangements*

	Floor	***Size*** $[cm^2]$	***Longitudinal bars***	***Stirrups***
Beams	1st,2nd, 3rd	40x50	5 $\phi_u 18$+ 3 $\phi_i 18$	2-leg ϕ8/10 (D), 2-leg ϕ8/15 (ND)
	4th,5th	40x50	4 $\phi_u 18$+ 3 $\phi_i 18$	
Columns	all	60x60	12 ϕ20	4-leg ϕ8/10
Nodes	all			2-leg ϕ8/5

All the structural reinforcement arrangements of the building, including the cross-section of two beam arrangements, along with the length of the bars and their respective overlapping are better represented in Figure 7.2**,** taken from Miceli and Castaldo (2024)**.**

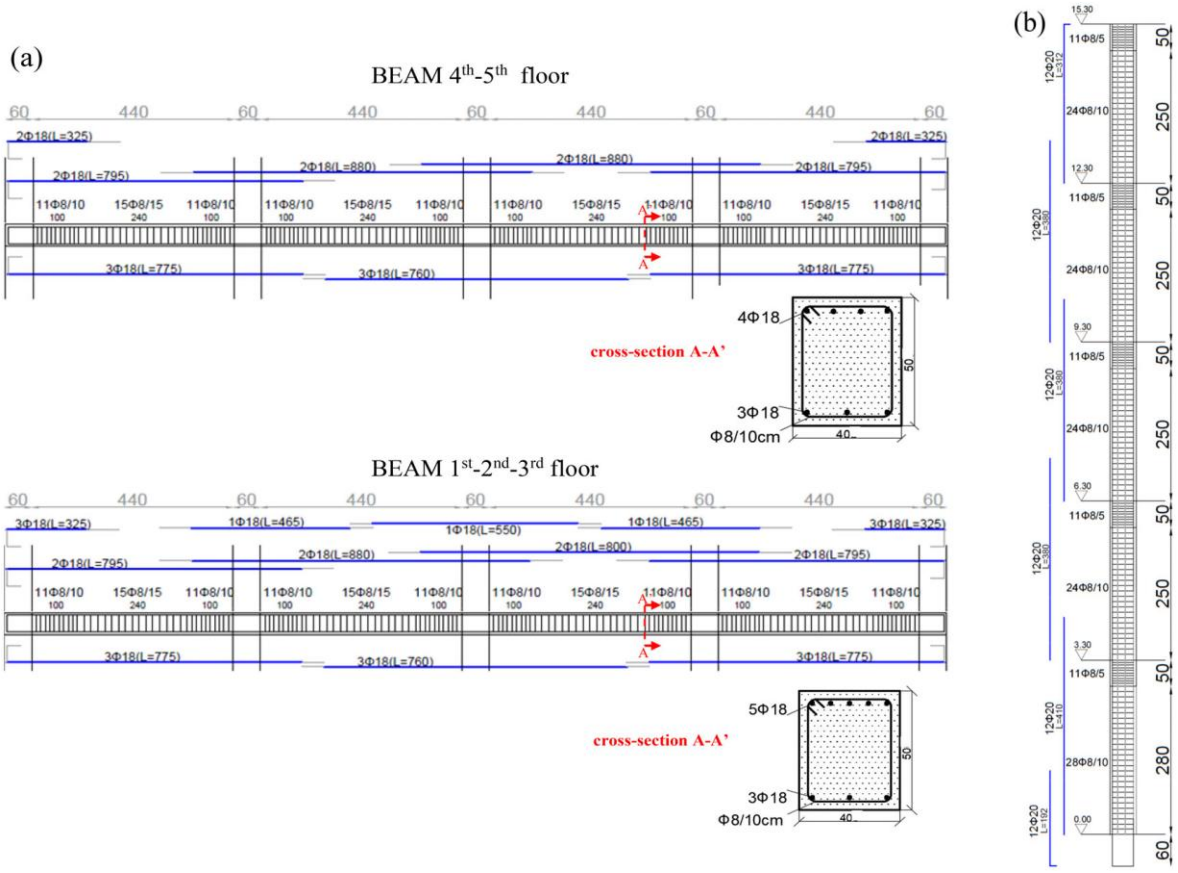

Figure 7.2 *Reinforcement structure arrangements (Miceli and Castaldo, 2024)*

7.2. FEM modeling

The execution of this thesis is based on the use of a model developed in finite element method software, which allows studying the nonlinear response of reinforced concrete frames considering both brittle and ductile mechanisms.

In particular, the model is developed using the software ATENA 2D v5, produced by Cervenka Consulting, where a bidimensional analysis is performed. This approach is chosen due to the need to improve the design of plane frames from a robustness perspective.

The geometry of the model is built step by step, following a structured approach. A brief description of the process is as follows:

The first step is to establish the important reference points, such as the start and end of each element, as well as the locations for longitudinal and transverse reinforcement, later the defined points are then connected using curves, following a logical sequence that ensures a coherent and meaningful numbering of the elements.

After this, closed sections are defined as macro-elements, where the model distinguishes four different concrete areas: Dissipative Area (Beam D, these sections are designed for plastic energy dissipation and are subjected to high inelastic deformations), Non-Dissipative Area (Beam ND, these remain mostly elastic during seismic or extreme loading events), Column Area, Concrete Cover Area (which remains the same for all cases). Each of these four macro-elements are assigned to a specific material type with the same name.

Other materials used in the model include reinforcement steel, plates, and springs, which will be discussed in detail later. Finally, curves are generated and assigned as steel reinforcement, ensuring an accurate representation of the structural behavior.

The model is performed using a quadrilateral finite element named "*CCIsoQuad*", which according to Cervenka (2021), is an isoparametric element with bilinear interpolation and Gauss integration at four integration points.

Previously, the cross-section of the building was described, but since the model is analyzed in 2D, the section dimension of the elements is 50 cm for the beams and 60cm for the columns. Additionally, the mesh size is 0.1 m, a size that ensures numerical accuracy for the assessment.

The model is solved using the standard Newton-Raphson iterative procedure, where load increments are fixed, and displacements are iterated until equilibrium is reached. The convergence criteria are introduced with a maximum 2000 iteration for step, and following the states given in Miceli and Castaldo (2024), the tolerances are:

- 1.0% for displacement norm error.
- 1.0% to 2.5% for the residual force norm error.
- 1.0% to 2.5% for the maximum residual force error.
- 1.0% for the out-of-balance energy error.

The concrete es modeled as "*Sbeta material"* for a nonlinear behavior, according to Cervenka (2021), "the formulation of constitutive relations is considered in the plane stress state, and a smeared approach is used to model the material properties, such as cracks or distributed reinforcement"

In tension, the response remains linear elastic (with elastic modulus E_c) until the tensile strength (f_t) is reached. After cracking, tension stiffening is considered using a linear softening approach based on local strain. The

descending branch of the stress-strain diagram is defined by the strain c3 corresponding to zero stress, as is shown in Figure 7.3.

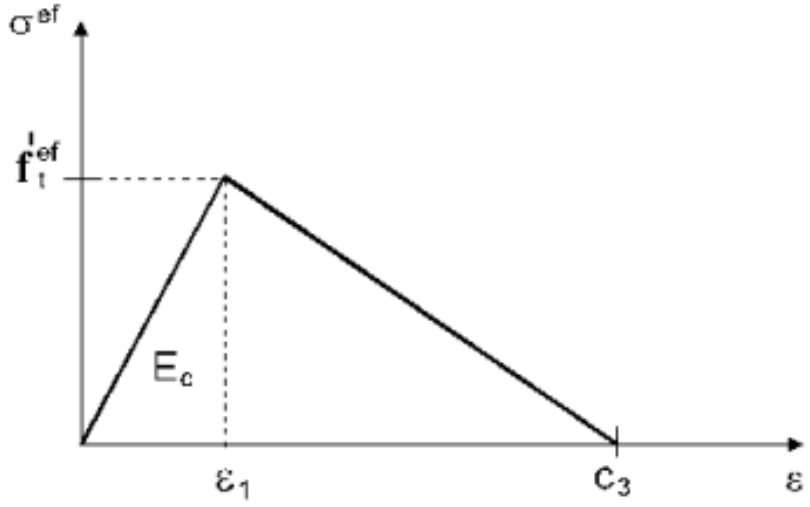

Figure 7.3 *Linear softening based on strain (Cervenka, 2021)*

In compressive behavior follows the CEB-FIP Model Code 90 for the ascending branch of the concrete stress-strain law, This formula allows wide range of curve forms, from linear to curved, and is represented by Figure 7.4, where E_c is secant elastic modulus at peak stress, ε_c peak strain, and f_c is compressive strength. The post-peak softening branch is modeled with a linear descending law. Lastly, the shear modulus is reduced after cracking, and this is modeled using a variable shear retention factor.

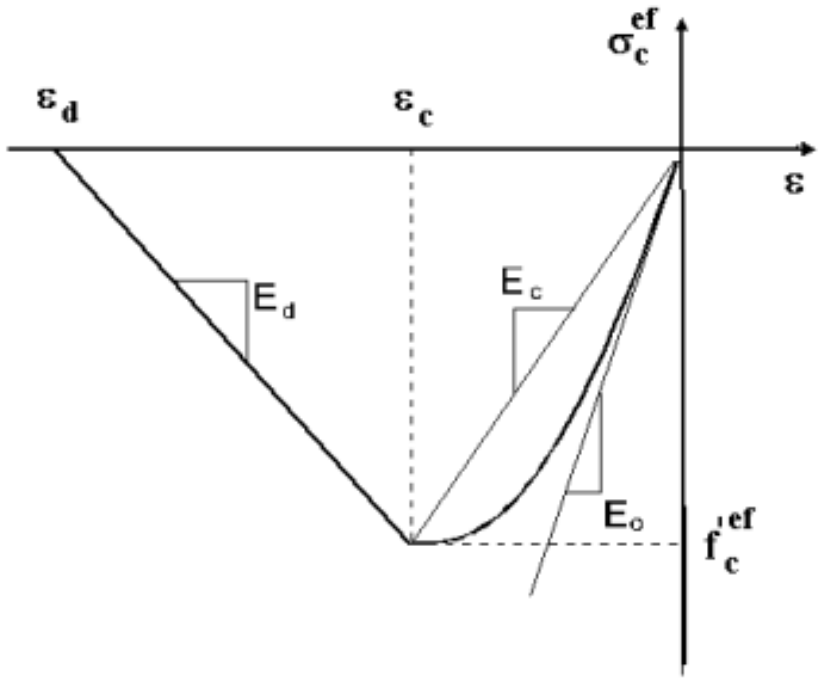

Figure 7.4 *Compressive stress-strain diagram (Cervenka, 2021)*

The reinforcement material used is *B450C steel*, modeled as discrete truss elements with perfect bond assumption with the concrete. The material follows a bilinear stress-strain law, with hardening in both tension and compression, assuming elastic-perfectly plastic behavior as shown in Figure 7.5, where E_s is the elastic modulus of steel and E_{sh} is the hardening modulus, which represents the plasticity of steel with hardening.

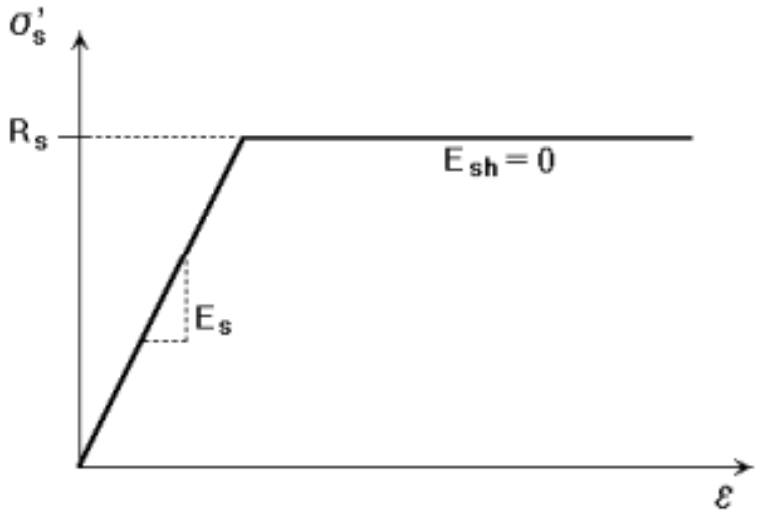

Figure 7.5 *Bilinear stress-strain law (Cervenka, 2021)*

Finally, the building is modeled with 3 load cases. The first one consists of fully fixed constraints at the column bases, the second one is the self-weight of the building, and the third one is the imposed displacement of 1 cm each step at the removed column's location.

A plate of 5 cm is added on top of the lost column to redistribute stress, Additionally, two monitoring points are placed, one measuring displacement at the middle of the plate and another at the top of the plate, relative to the reaction.

On the other hand, as mentioned by Miceli and Castaldo (2024), the vertical imposed displacement allows performing a displacement-controlled Nonlinear Finite Element (NLFE) pushdown analysis. This method enables tracking of:

- Load-deformation response.
- Crack propagation patterns.
- Stress distribution and damage localization.
- Residual resistance and capacity curve analysis.

This approach allows evaluating the frame's progressive collapse resistance and understanding how it transitions from flexural to catenary action.

A representation of the how the model sees in ATENA 2D v5 with the macro-elements and lines is shown in Figure 7.6.

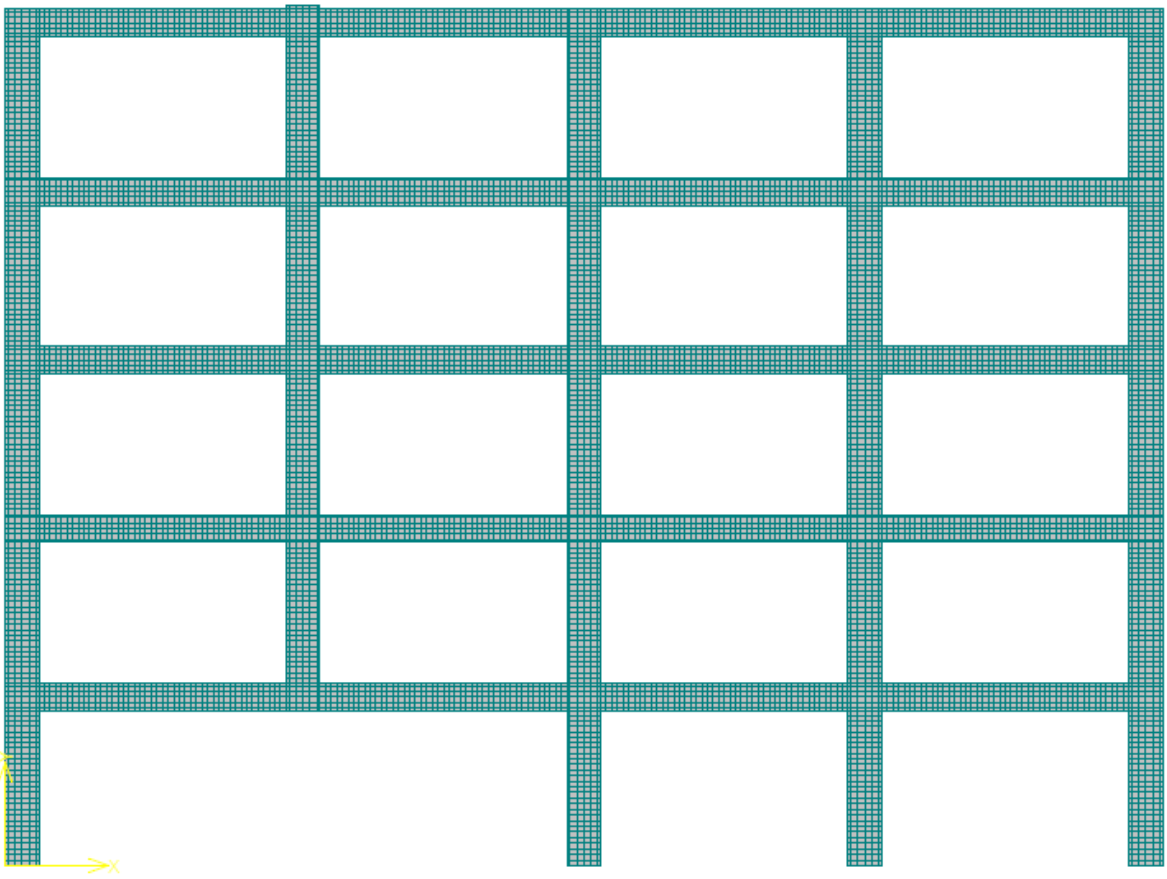

Figure 7.6 *Model in ATENA 2D v5*

7.3. Equivalent springs

The equivalent springs are used to simulate the contribution of orthogonal structural elements, which would be present in a 3D building. Specifically, these translational springs represent the effect of transverse beams and slabs in restricting the lateral displacements of a specific plane frame due to their stiffness, by that means improving the structural robustness.

According to Zheng et al. (2022), the horizontal stiffness values of each spring can be computed using a linear elastic analysis, assuming that the horizontal stiffness remains fully elastic. In this way, a unitary axial force ($K = 1kN$) is applied in the in-plane direction of the studied frame to obtain the corresponding displacement (δ) at the node. The equivalent spring stiffness (K) is determined as the ratio between the applied force and the measured displacement:

$$K = \frac{F}{\delta}$$

Miceli and Castaldo (2024) performed this analysis using SAP2000 on a 2D frame with the failure scenario of second-to-last column removal failure scenario, a structure like the assessed in this thesis, and the horizontal stiffness values obtained are shown in Table 7.3. Here, it is possible to observe how the horizontal stiffness on the beams decreases in a non-linear way from the initial floor to the last floor, this has a direct implication on the collapse behavior of the structure.

Table 7.3 *Equivalent Spring stiffness (Miceli and Castaldo 2024)*

	Spring Stiffness Column A [N/m]	***Spring Stiffness Column C [N/m]***	***Spring Stiffness Column B' [N/m]***	***Spring Stiffness Column A' [N/m]***
1st floor	7.468E+06	9.747E+07	1.685E+08	9.766E+07
2nd floor	7.210E+06	7.128E+07	1.031E+08	7.138E+07
3rd floor	6.954E+06	5.283E+07	6.854E+07	5.288E+07
4th floor	6.684E+06	4.119E+07	5.013E+07	4.120E+07
5th floor	6.309E+06	3.288E+07	3.837E+07	3.289E+07

The equivalent springs are modelled and applied at the center line of each beam-column node in ATENA 2D v5 and its representation is seen in the model as is shown in Figure 7.1.

8. Robustness improvement and assessment

8.1 Design Improvement

As mentioned in Section 3, several standard codes propose strategies to ensure structural robustness. For example, the Eurocode suggests improving the design of key elements, designing structural components with sufficient ductility, and incorporating structural redundancy to enhance load transfer through alternative paths.

Since structural robustness has been a topic of growing interest in the last decades, various authors have studied and proposed different strategies to improve the behavior of structures in case of the loss or failure of critical structural elements. These strategies generally recommend additions or changes to the arrangement of the section reinforcement.

Miceli and Castaldo (2024) consider some improvement strategies proposed in design codes, particularly section symmetry and continuity in supports, strategies initially proposed by GSA (2003)

- *Section symmetry*: This refers to the symmetrical arrangement of structural elements, ensuring that the amount of reinforcement steel is the same in the compression and tension zone of the element. This guarantees balanced behavior under accidental loads. In the case of loss of a structural element, such as a column, a symmetric section facilitates a uniform load distribution and contributes to greater ductility

and load capacity, considering the change in sign that occurs in the beam bending moment during such event.

- *Support continuity*: This refers to the importance of appropriate connection of the structural elements at beam-column nodes, making possible the load transfer in case of support failure and allowing the development of catenary mechanisms. In this context, it is essential to design strong and ductile connections between beams and columns, ensuring higher amount of reinforcement in high-stress areas.

As mentioned in section 7.3, the inclusion of equivalent springs that simulate the presence of transverse structural elements which is achieved through lateral restraints at the frame nodes.

New Proposals

Taking the previous considerations into account, Miceli and Castaldo (2024) have proposed new design strategies to improve structural robustness, which include:

- *Continuity*: This criterion is inspired by the principle of support continuity but increases the length of beams longitudinal reinforcement by up to 30 %, additional to the anchorage length. This additional length is justified in the event of the loss of a support element because the distribution of the bending moment changes significantly, extending into the top chord of the beam. Preventing the formation of plastic hinges in transverse sections with lower strength and ductility.

- *Global floor equality*: This strategy proposes applying the same amount of reinforcement in all the floors, using the reinforcement arrangements of the lower floor as reference because reinforcement arrangements in lower floors are usually greater due to the higher internal actions generated by seismic combinations. When structural support is lost, the high axial stiffness of the columns generates a uniform load distribution across all floors. Additionally. It can be assumed that the floors displacement is similar, which can be explained by the Vierendeel behavior in the beams.

- *Side face rebar*: This strategy suggests adding longitudinal reinforcement bars on the lateral side of the beam. Due to their location near to the barycenter section, these bars are not subject to significant stress in the initial phase. However, when the beam enters the softening stage and is subject to higher tensile forces, the lateral bars help to reduce mechanical stress, thereby improving the structure's ability to redistribute loads. This enhances the tying effect and activates the catenary behavior.

To make the following description easier, the previous improvement strategies will be named as *C* for continuity, *S* for section symmetry and *E* global floor equality.

8.2 Pushdown analysis modelling

Considering the parameters established in the previous section, the pushdown analysis is performed to evaluate the capacity curve of the structure which its second-to-last column has been removed as is shown in Figure 7.1.

According to Miceli (2024), this analysis assesses structural resistance by applying an increasing vertical displacement imposed statically at the point where the column was removed. It is important to mention that applying an imposed displacement instead of a load allows evaluation of the structural softening response. Additionally, in this stage of the analysis external loads are not applied, only the concentrated displacement is considered, which is an assumption.

This evaluation is carried out until the collapse of the structure occurs, which can happen due to failure of the concrete at its maximum strength or reaching the ultimate strain of steel reinforcement bar.

This thesis considers a single failure scenario but evaluates the structural response in three different cases. In each case, the structure maintains the cross-section geometry and element properties, but the reinforcement design varies, and more specific details of each case will be described later.

For each of the three frames evaluated, 100 models for each frame were executed, introducing variations in the fundamental parameters and applying the uncertainties concepts mentioned in Section 5.2, and further explained in

Section 9.1. Due to this variability, each model exhibits a different structural response, leading to different results. The results obtained in each case are analyzed based on their capacity curve and whether they exhibit a catenary behavior under the given conditions.

8.2.1 Frame 1- Standard model + springs

The first structural case corresponds to the one described in the previous section. In this case, the building is designed according to current standard codes (NTC 2018 and Eurocode). This structure is designed taking into account two strategies of improvement suggested in Section 8.1, these are continuity and the inclusion of equivalent lateral springs.

The reinforcement arrangements for the columns consist of 12 ϕ20 bars, with transverse reinforcement of 4-leg ϕ8 spaced each 10 cm along the whole column, while at the beam-column nodes, the spacing is 5 cm.

Regarding the beams, the longitudinal reinforcement at the higher stressed section is 3 ϕ18 bars in a bottom chord in the five floors, while for the upper chord, the longitudinal reinforcement is 5 ϕ18 bars for the first three floors and 4 ϕ18 bars for the 4^{th} and 5^{th} floors. The transverse reinforcement is done of 2-leg stirrups, spaced 10 cm in the dissipative zone and 15 cm in the non-dissipative zone. The reinforcement arrangement for frame 1 is shown in Figure 8.1.

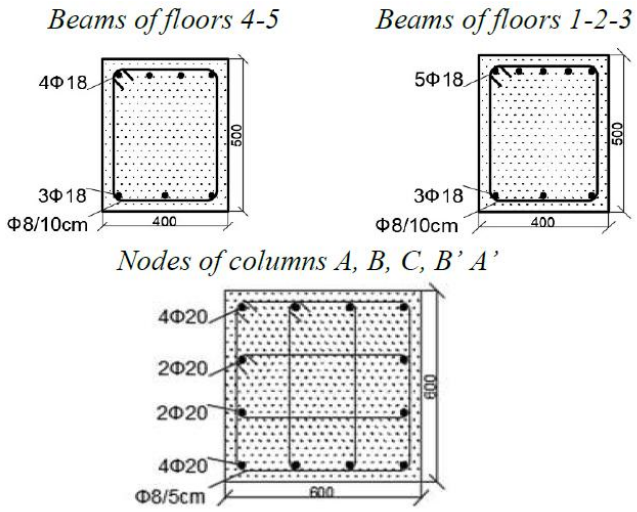

Figure 8.1 *Reinforcement arrangement for the frame 1(Miceli et al., 2025)*

According to Figure 8.2, which shows the capacity curve of frame 1, it is possible to describe the structural behavior as follows:

Frame 1 manifests softening behavior, where the curves reach their maximum load capacity and then shows a slightly ductile response. As the load decreases, the structure continues to deform until it finally collapses. The maximum value of load in the flexural stage is approximately $P_{max} = 980\ kN$. The figure suggests that the displacement at the peak load is around 0.04 m, which remains closely similar in all iterations. However, the ultimate load does not show a clear pattern, assuming that collapse occurs at a displacement of 60 cm in all cases ultimate load in most simulations is approximately $P_{ult} = 350\ kN$.

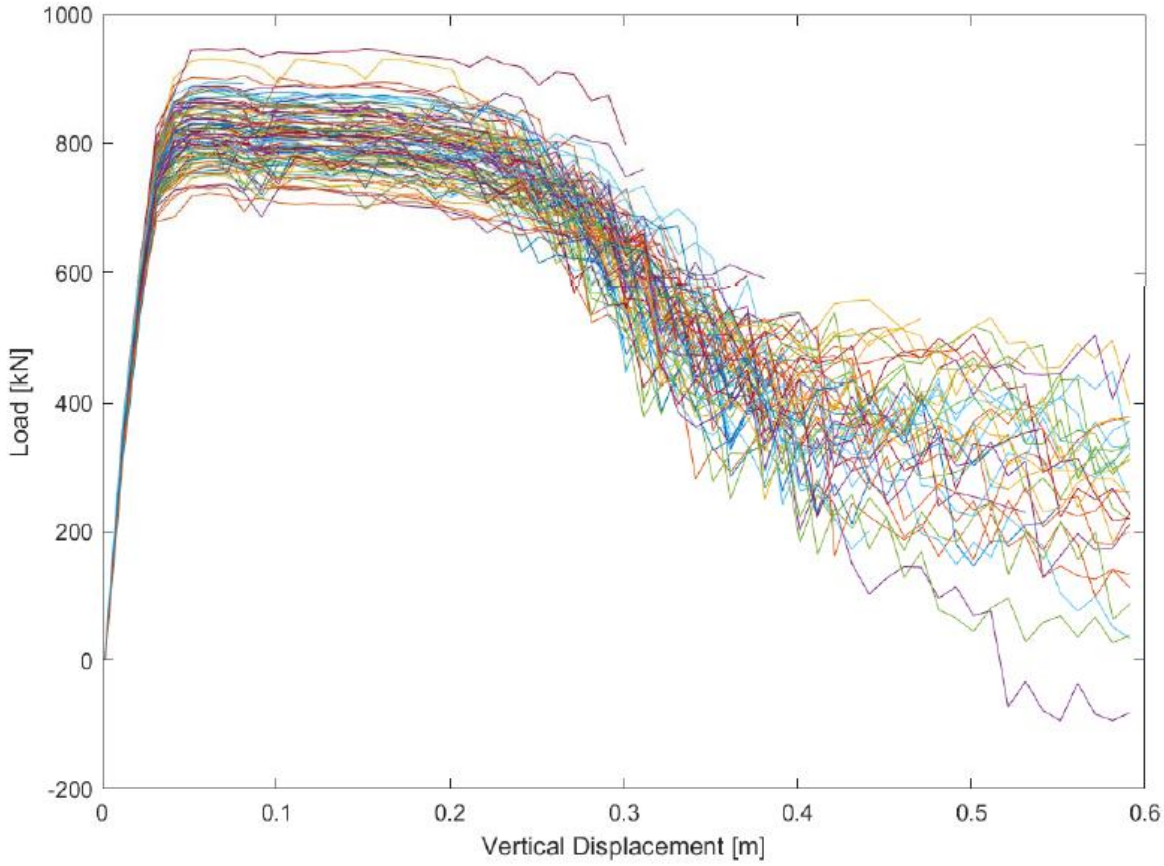

Figure 8.2 *Capacity curve frame 1*

8.2.2 Frame 2- C+ Side face rebar+ Springs

The structural design has been modified to enhance the building's robustness. Considering the new proposals by Miceli and Castaldo (2024), the concept of continuity is applied to the structure. This involves extending the length of the longitudinal steel reinforcement by 1.5 m in each direction of the span.

Additionally. The side face rebar strategy is implemented by adding 2ϕ16 bars on each lateral side of the beam, located approximately at 1/3 and 2/3 of the

beam height. As in the previous structure, the equivalent lateral springs are also considered.

The reinforcement arrangement for higher stressed section in this structure is close simitar to the previous case, with only two modifications, the addition of the side face rebar, as was said before, and the reduction to 7.5 cm the spacing for the 2-leg ϕ8 stirrups in the dissipative zone of the beams, this to comply with seismic verifications requirements.

For the columns and beam-column nodes, the reinforcement remains unchanged from the previous. The reinforcement arrangement for the second case is shown in Figure 8.3.

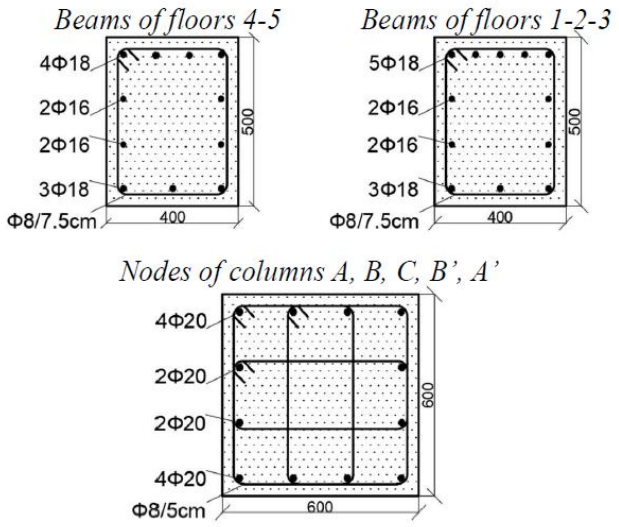

Figure 8.3 *Reinforcement arrangement frame 2 (Miceli et al., 2025)*

According to Figure 8.4, which shows the capacity curve of frame 2, it is possible to observe how the structure exhibits a different behavior compared to frame 1. The value of peak load is higher in all cases, nevertheless, the

ultimate load does follow a clear pattern. In some iterations, the ultimate load value is higher than the peak load, which would suggest a catenary behavior of the structure, but in some iterations the structure still has a softening behavior.

From Figure 8.4, it is possible to assume that the maximum value of peak load at flexural stage is approximately $P_{max} = 1400\ kN$. Similar to frame 1, the displacement at peak load stays relatively constant at around 0.6 m.

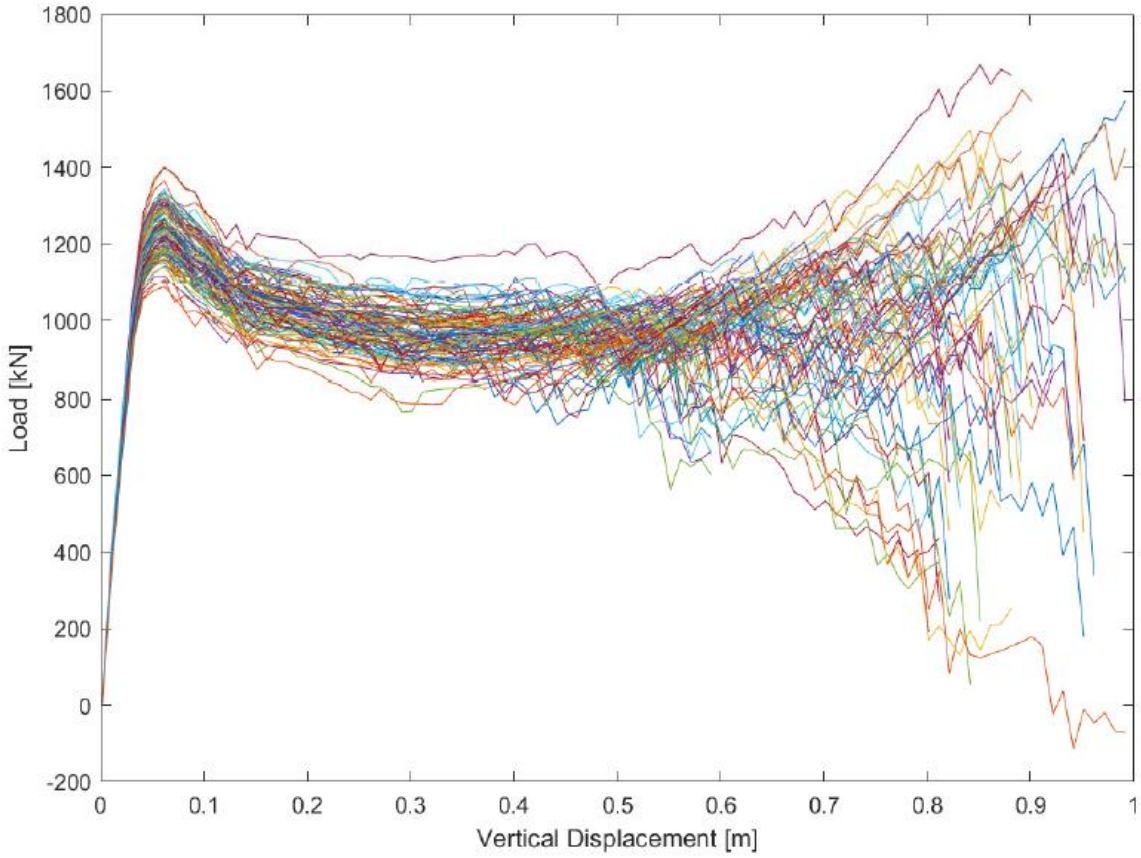

Figure 8.4 *Capacity curve frame 2*

8.2.3 Frame 3- CSE + Side face rebar+ springs

This case derives from the previous one, where part of the strategies proposed by Miceli and Castaldo (2024) were already considered. However, in addition to those, the remaining proposed strategies are applied, incorporating the section symmetry and the global floor equality.

Regarding the section symmetry, the beams have the same longitudinal reinforcement in the upper and lower chords. Concerning global floor equality, the reinforcement arrangement is the same on all floors. Taking as reference the reinforcement of the top chord of the first floor, which is the section subject to higher stresses. The reinforcement arrangement of the structure consists of 5ϕ18 bars in the upper and bottom chords of the beam, with 2ϕ16 bars on the lateral sides of the beam, this for the five levels.

To conserve the capacity design principles and respect the strong column-weak beam principle, the spacing of the stirrups in the dissipative area of the beams is reduced to 7.5 cm. Additionally, for the beam-column nodes, the diameter of the stirrups is increased to ϕ10 with the same spacing of 5 cm. Regarding the columns and beams in the non-dissipative area, the reinforcement design remains the same. A representation of the reinforcement arrangement of the third structure is shown in Figure 8.5.

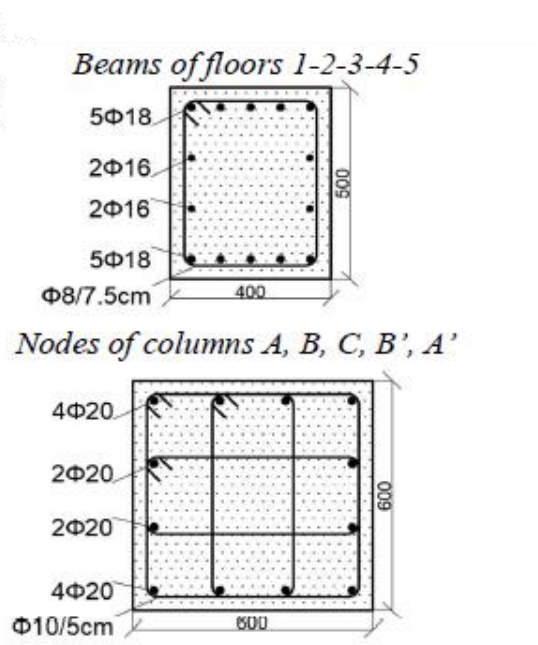

Figure 8.5 *Reinforcement arrangement frame 3 (Miceli et al., 2025)*

According to Figure 8.6, which shows the capacity curve of frame 3, it is possible to observe that the curves are closely similar to those of frame 2, but the maximum value of peak load is higher. Additionally, the behavior of the ultimate load tends to be relatively equal to the peak load and, in many cases, the ultimate load is higher than the peak load. This suggests that the structure exhibits catenary behavior, where the vertical displacement increases and the reaction load also increases, showing a clear nonlinear response.

From Figure 8.6, it is possible to assume that the maximum value of peak load is approximately $P_{max} = 1700\ kN$, as in the previous frames is consider that the displacement at peak load is remains the same for all the cases,

around 0.06 m. Additionally, it is possible to suggest that the maximum value of the ultimate load in one of the iterations is approximately $P_{ult} = 2400\ kN$.

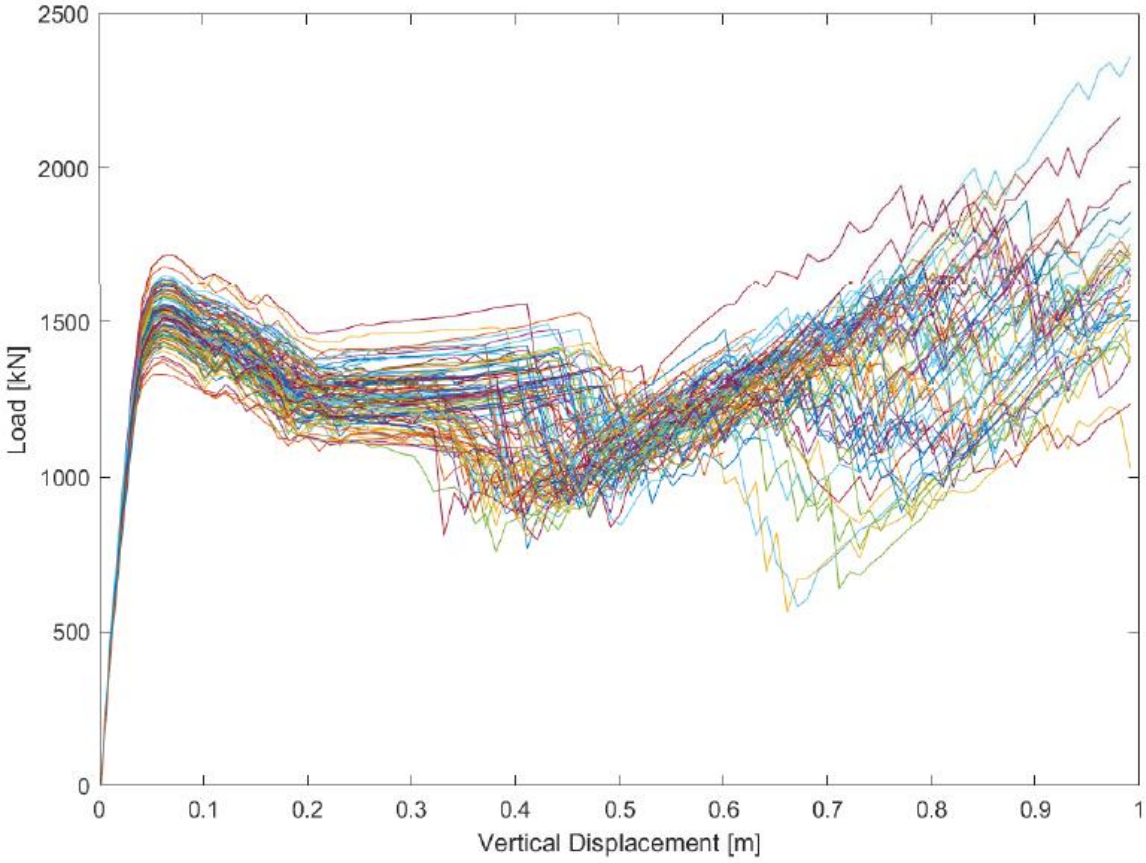

Figure 8.6 *Capacity curve frame 3*

9. Structural reliability of the frames

Finally, this chapter describes the procedure to achieve the main goal of this thesis, evaluating the structural reliability against the progressive collapse, considering it as the probability of failure of the previously described scenario. For this reason, each variation made to the structure corresponds to a case study.

This work follows the procedure proposed and applied by Miceli et al. (2025), who to assess structural robustness in terms of reliability has used a fully probability approach. This procedure follows the next five steps.

9.1. Sample the aleatory properties of materials and loads

The random properties of material parameters and load variation are obtained using the *Latin hypercube sampling* (LHS) technique. According to Mckey et al. (1979), the LHS method divides the range of each input variable X into N strata of equal marginal probability ($1/N$) and selects a random value from each stratum. Then, these values are randomly combined among the variables to form the final samples. This approach ensures that each variable is stratified across its entire range, which is particularly useful when the output strongly depends on only a few variables.

For this analysis, the test is conducted using the software MATLAB, which has a specific command that carries out the LHS test, for this scenario has been generated eleven basic random variables associated with five parameters corresponding to material properties and six variables related to applied actions on the structure.

The sample variables are:

Material properties

- Concrete compressive strength f_c
- Reinforcing steel yielding strength f_y
- Reinforcing steel ultimate strength f_u
- Reinforcing steel elastic modulus E_s
- Reinforcing steel ultimate strain ε_{su}

Variable for actions

- Reinforced concrete specific weight ρ
- Permanent structural load G_1
- Permanent non-structural load G_2
- Floor variable load G_f
- Roofing variable load G_r
- Snow load G_s

The mean value, distribution type and coefficient variation of the parameters sampled by the LHS test are presented in Table 9.1, with the values provided by Miceli et al. (2025).

The number of samples generated is 100, a quantity selected to ensure a stable estimation between the variance and the mean of the resulting variables, as stated by Mckey et al. (1979, cited in Miceli,2024).

Table 9.1 *Characteristics of the sampled basic variables (Miceli et al., 2025)*

	Distribution type	***Mean Value***	***Coefficient of variation***
f_c	*Lognormal*	*31.9 MPa*	*0.15*
f_y	*Lognormal*	*210000MPa*	*0.03*
f_u	*Lognormal*	*488.6 MPa*	*0.05*
E_s	*Lognormal*	*589.8 MPa*	*0.05*
ε_{su}	*Lognormal*	*0.14*	*0.09*
ρ	*Normal*	*25* kN/m^3	*0.05*
G_1	*Normal*	*16* kN/m	*0.05*
G_2	*Normal*	*13* kN/m	*0.05*
G_f	*Gumbel*	*7.3* kN/m	*0.2*
G_r	*Gumbel*	*1.8* kN/m	*0.2*
G_s	*Gumbel*	*4.7* kN/m	*0.2*

In this context, each variation of the parameters generates a new random structure, which in each iteration maintains the same geometry and design as the corresponding case of study, but the material parameters vary according to each LHS iteration. It is important to note that the LHS test was executed only once, and the generated values were applied to each of the three frames of studies.

9.2. Perform a Pushdown analysis

The evaluation of the building's structural response is performed by imposing a progressively increasing vertical displacement through a non-linear finite elements analysis. This assessment is carried out using a pushdown analysis, in which a column is removed, and imposed vertical displacement is applied at the location of the removed column.

During the analysis, both displacement and the reaction are monitored step by step, allowing the capacity curve of each random structure to be obtained. This capacity curve will be used to determine the corresponding values of dynamic displacement and load.

A complete description of the executed procedure, along with the analysis of the capacity curves obtained is presented in Section 8. On the other hand, Figure 9.1 provides a graphical representation of the structural deformation after performing the pushdown analysis of frame 2 with a scalar multiplier of 2, furthermore cracks of structure are visible.

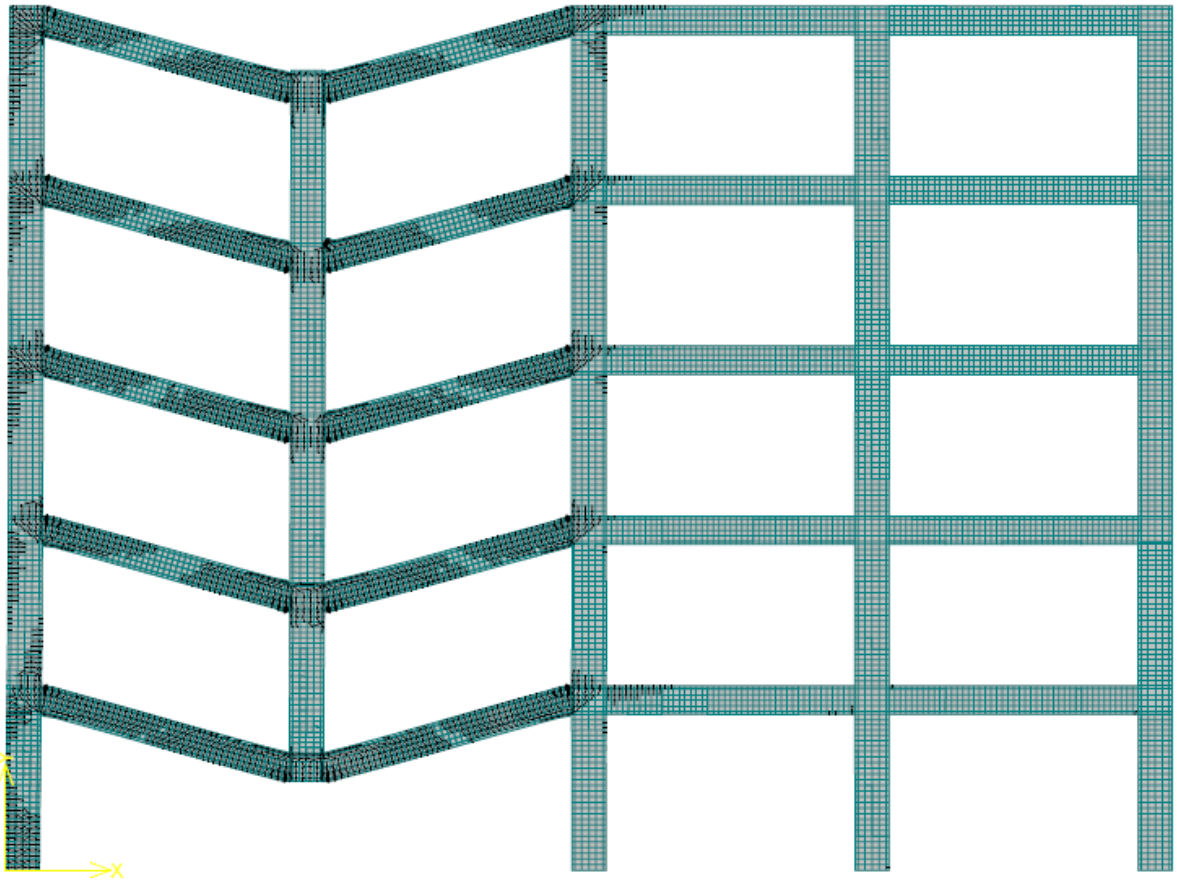

Figure 9.1 *Behavior of the frame under pushdown analysis*

9.3 Compute the dynamic amplification factor (DAF)

To determine the *dynamic amplification factor* (DAF), the energy equivalence approach is used, like is suggested by Izzudin (2008). The central idea of this method is that the sudden loss of a column is analogous to the sudden application of gravity loads on the affected substructure. After this loss, the structure undergoes a non-linear dynamic response. In the initial stage, the gravitational load exceeds the static resistance of the structure, causing an increase in deformation, which is transformed into an increase in kinetic

energy, thus increasing the velocity of the structure. As deformations increase, static resistance also increases until it oversteps the gravity loads, reducing the kinetic energy.

Finally, the maximum displacement is reached when the kinetic energy is reduced to zero, which occurs when its derivation is zero, and therefore, the velocity becomes zero again. Thus, the phenomenon occurs when the work done by the external gravity loads *W* is equal to the energy absorbed by the structure *U*, thus determining the dynamic displacement. The above can be expressed with the following formulas.

$$W = \lambda_d P_0 u_d$$

$$U = \int_0^{u_d} P(u)du$$

The external work *W* is calculated by multiplying the static gravity load P_0 at the point where the column was removed by the vertical displacement at the same point. Meanwhile, the internal energy is obtained by evaluating the area under the capacity curve up to the dynamic displacement. Izzudin (2008) illustrates this principle with Figure 9.2

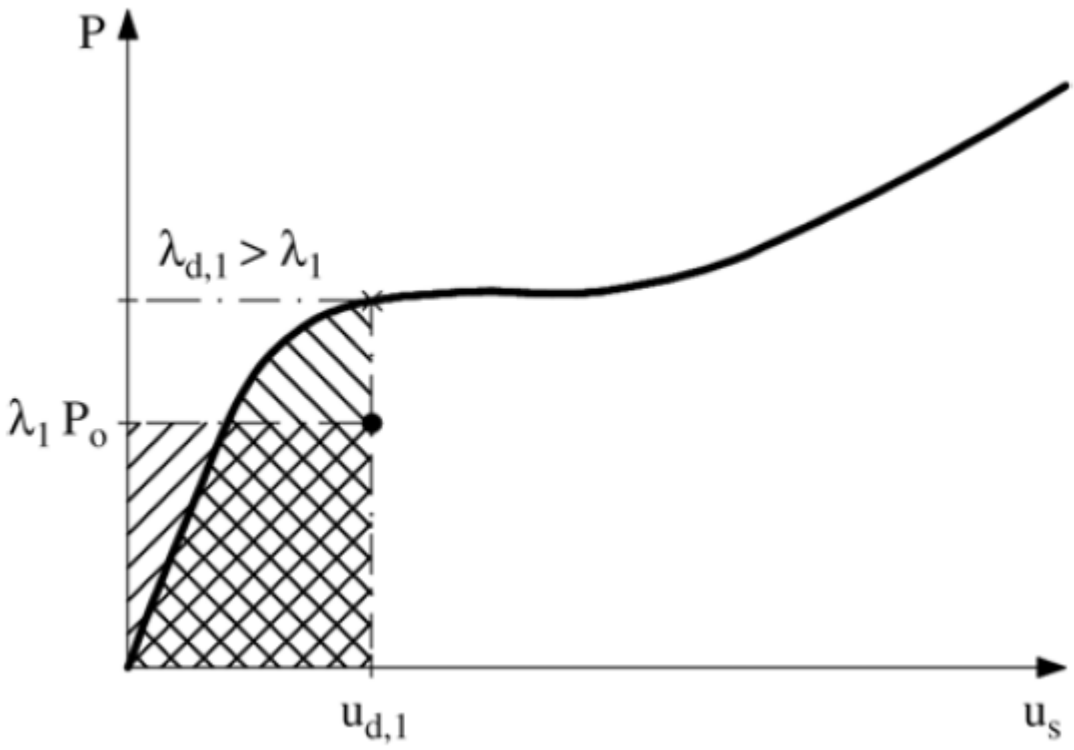

Figure 9.2. *Dynamic response. (Izzudin, 2008)*

Additionally, by equating external work with internal energy, it is observed that the value of the dynamic amplification factor is given by the ratio between dynamic gravity load P_d and static gravity load P_0.

$$\lambda_d = \frac{P_d}{P_0}$$

The value of the static gravity load P_0 is determined by calculating the work done by the external gravity loads, obtained from the product of the distributed load and the effective length of the span, with the objective of finding the concentrated force applied at the column removal point. Since external gravity loads do not depend on internal variations in the structural design, they

remain constant for the three frames studies, considering only their variation in each iteration of the LHS test.

The value of dynamic gravity load P_d is determined from the results of the capacity curves obtained in the pushdown analysis performed in step 2. The dynamic load is represented by the value on the capacity curve corresponding to the dynamic displacement, which is obtained from the intersection between the external work and the internal energy of the structure.

In the evaluation of this intersection, two possible cases may arise:

- Case 1: It is not possible to find an intersection point between the external work and the internal energy; this indicates that the external work is always greater than the internal energy available in the structure, as shown in Figure 9.3. This means that the structure is unable to withstand the accidental removal of the column, making it impossible to calculate a value for the dynamic amplification factor.

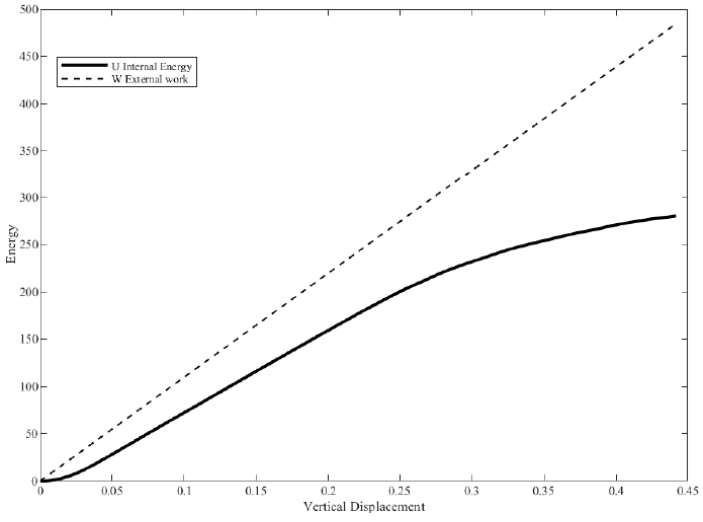

Figure 9.3 *Not energy equivalence*

- Case 2: Represented by Figure 9.4, the point where external work and internal energy are equal is observed. Graphically, this is represented as the intersection of the curves, this intersection point defines the dynamic displacement, and in these cases, it is possible to calculate the dynamic amplification value.

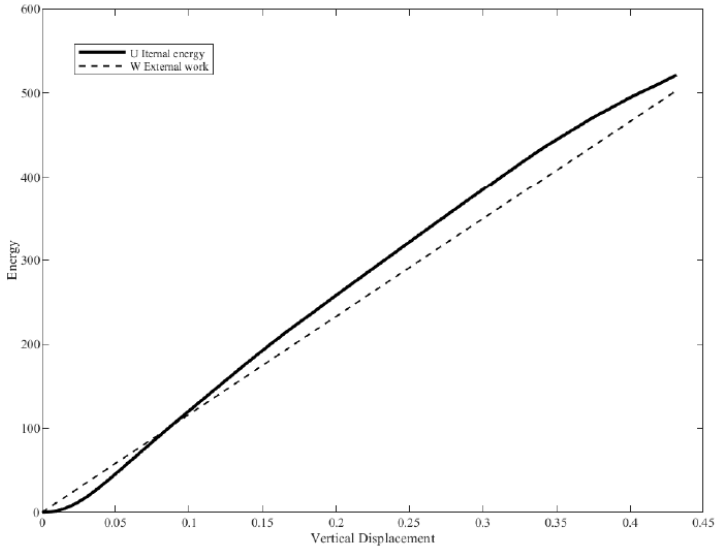

Figure 9.4 *Energy equivalence*

Analyzing the results of the Dynamic Amplification Factor (DAF) obtained in MATLAB, it is possible to conclude that for most of the iterations in frame 1 a DAF could not be determined, this is because external work is usually greater than internal energy, meaning that the external load applied to the structure is higher than the energy that can be. This suggests that frame 1 will collapse in majority of iterations.

For frame 2, the Dynamic Amplification Factor could be determined in 47 % of the iterations, with a mean value of $\lambda_d = 1.196$, and a standard deviation of 0.108. Furthermore, it is interesting to note that the maximum and minimum value for the DAF are $\lambda_{d,max} = 1.452$ and $\lambda_{d,min} = 1.007$, respectively.

For frame 3, the Dynamic Amplification Factor was found in almost all the iterations, where only 4% of the iterations do not reach to find an intersection between external work and internal energy. The mean value of the DAF is $\lambda_d = 1.246$ with a standard deviation of 0.109. Additionally, the maximum and minimum value for the DAF is $\lambda_{d,max} = 1.551$ and $\lambda_{d,min} = 1.022$. respectively.

9.4 Perform an equivalent static analysis

In this step, a non-linear finite element equivalent static analysis is performed, where the removal of a supporting column is gradually simulated. Additionally, using the dynamic amplification factor obtained in the previous step, the gravity loads previously described and determined by Miceli (2024) based on the accidental load combination of the Eurocode are amplified.

This analysis is also performed in the software ATENA 2D v5 as the previous pushdown analysis. But in this case, the external gravity load influences into the analysis and are introduced into the model throughout of the section “load case”. Figure 9.5 illustrates how the loads are distributed within the model.

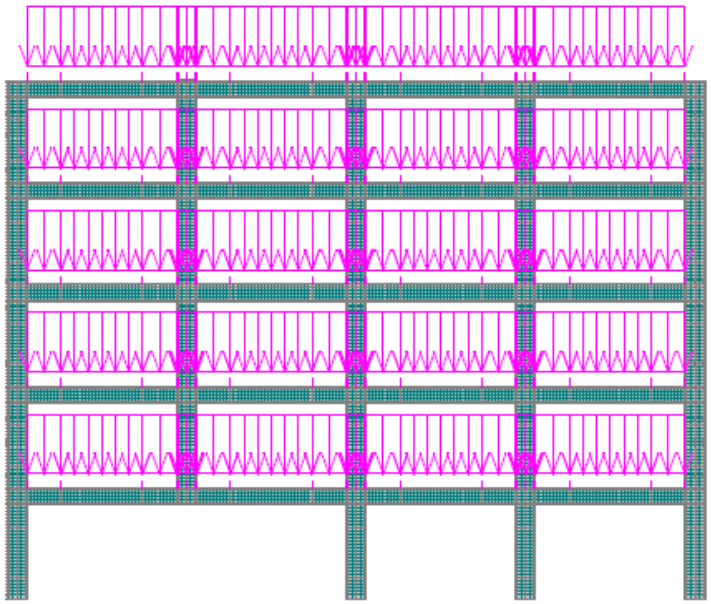

Figure 9.5 *Scheme of gravity loads*

Furthermore, the load amplification is applied only in the influence zone of the removed column, as shown in Figure 9.6. The progressive amplification of the load is carried out by adding steps in the “analysis steps” section.

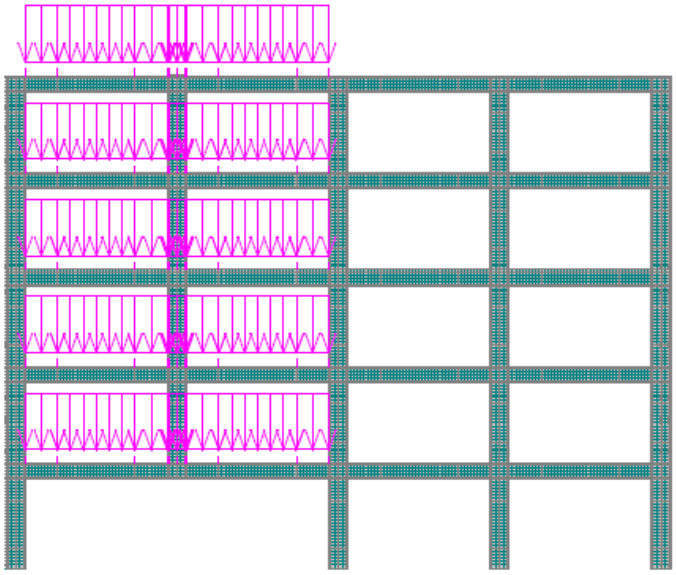

Figure 9.6 *Scheme of amplified loads*

The output of interest in these simulations is the *principal total strain* (ε_s) in the cross-section of the beam-column nodes. For analysis, specific points in the confined concrete core of the column and beam are analyzed, as well as the ordinary longitudinal reinforcement and transverse reinforcement, even though this last is not used for this thesis. In the case of frames 2 and 3, the side face rebar reinforcement is also examined. Figure 9.7 shows a representation of the point into the nodes that are evaluated.

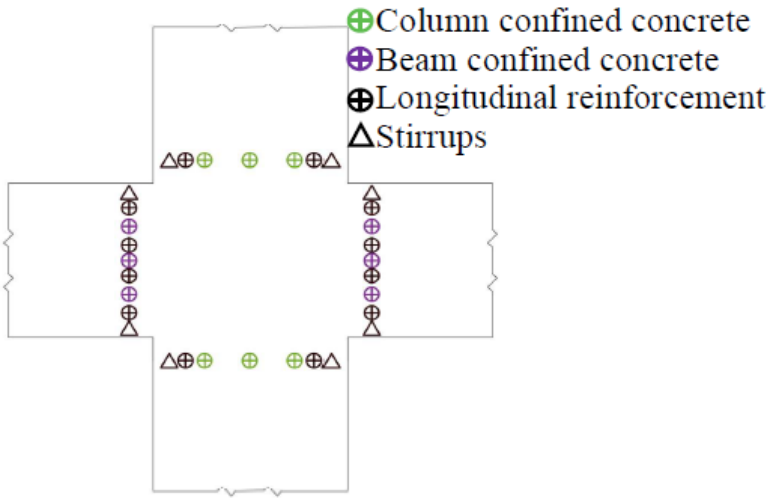

Figure 9.7 *Principal total strain analyzed points (Miceli, 2024)*

The results of the principal total strain are obtained for four sections of the beam-column nodes in the central zone, three sections in the lateral zones and the column removed point, and two sections in the upper corners of the structure.

9.5 Compute the probability of failures and structural reliability

Based on the output obtained in the previous sections, where the pushdown analysis and equivalent static analysis were performed using the ATENA 2D v5 software, the probability of failure of the structures is determined.

The probability of failure is defined as the probability that the random structural demand overpast the random structural capacity of the building. Considering that the structural demand *S* is obtained from the principal total strain of the points examined in the equivalent static analysis, while the structural capacity *C* is derived from the ultimate strain of the materials in the pushdown analysis.

The probability of failure due to local damage can be numerically evaluated through a convolution integral between the demand (expressed as a probability density function (PDF)), and the capacity (expressed as a cumulative density function (CDF)), following the described by Haldar and Mahadevan (2000), where $F_C(S)$ is the cumulative density function of the capacity, and $f_s(C)$ and $f_s(S)$ are the probability density function of the capacity and demand, respectively, as detailed by Miceli (2024).

$$p_f = P[C|LD] = P(C < S) = \int_0^\infty [\int_0^s f_C(c)\, dc] f_s(S) ds = \int_0^\infty F(c) f_s(S) ds$$

To determine the probability of failure in frame 1, it must be considered that in most simulations, it was not possible to find the dynamic amplification factor. In this context, the probability theorem is used as a reference, which serves

as the basis of the equation proposed by Jalayer and Cornell (2009). This equation calculates the total probability by considering two mutually exclusive events (collapse and not collapse), weighting their conditional probabilities. The corresponding equation is expressed below and is taken from Miceli (2024).

$$p_f = \frac{N_{non-collapse}}{N_{total}} \left[\int_0^{\infty} F(c) f_s(S) ds \right] + \frac{N_{collapse}}{N_{total}} * 1$$

The calculations mentioned above are repeated for the three case studies in each of the simulations, evaluating each point corresponding to specific material and each cross-section of the beam-nodes. The results obtained for the probability of failure are graphically represented on a structural frame drawn, where each node section shows a point with a color that represents a range of probability of failure, as shown in the following legend.

Legend:
- $0.58 < p_f < 1.0$
- $0.05 < p_f \leq 0.58$
- $10^{-3} < p_f \leq 0.05$
- $10^{-7} < p_f \leq 10^{-3}$
- $p_f \leq 10^{-7}$

The following representations highlight the computed values for the confined concrete and longitudinal steel reinforcement. It should be noted that some nodes do not have a color point in the results, this is because only the probability of failure for confined concrete in compression is shown, since confined concrete in tension is not a strong material at a high level of deformation.

The probability of failure for the confined concrete for frame 1 is shown in Figure 9.8, while the probability of failure for the longitudinal steel reinforcement is shown in Figure 9.9.

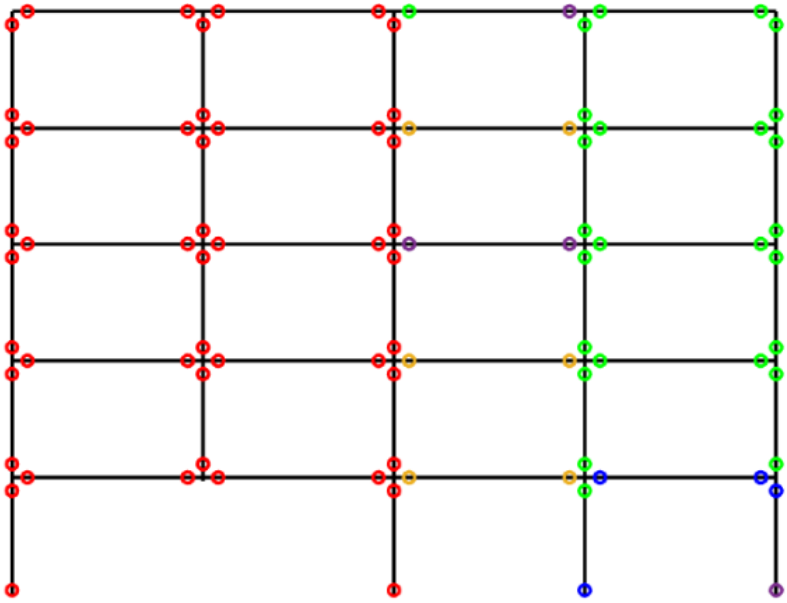

Figure 9.8 *Failure probability for concrete in frame 1*

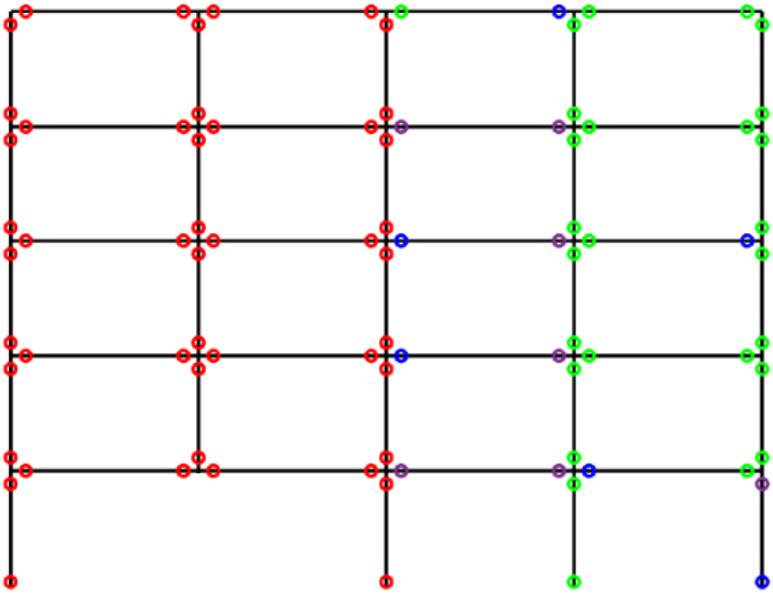

Figure 9.9 *Failure probability for steel reinforcement in frame 1*

The probability of failure for the confined concrete for frame 2 is shown in Figure 9.10, while the probability of failure for the longitudinal steel reinforcement is shown in Figure 9.11.

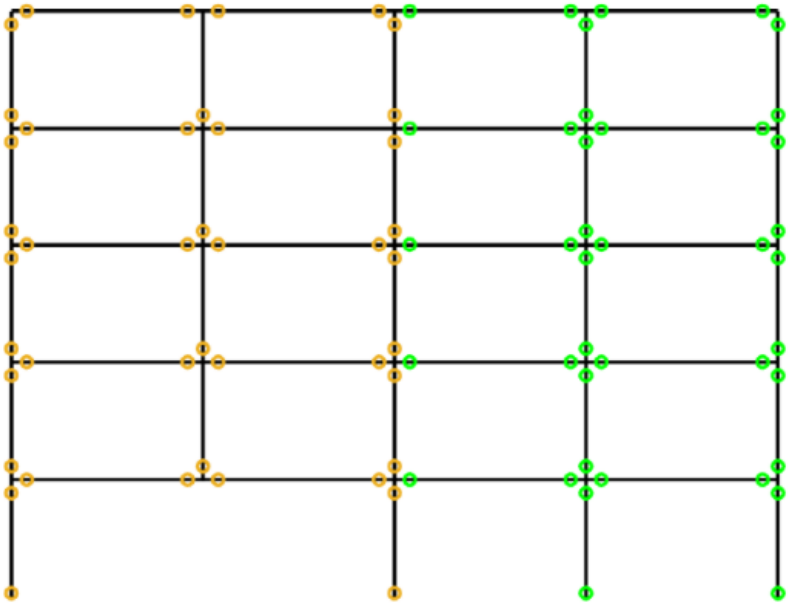

Figure 9.10 *Failure probability for concrete in frame 2*

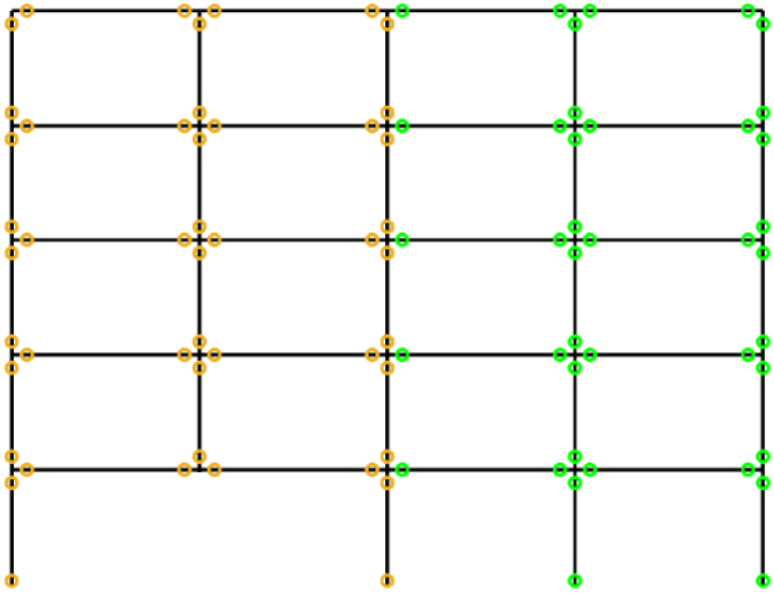

Figure 9.11 *Failure probability for steel reinforcement in frame 2*

The probability of failure for the confined concrete for frame 3 is shown in Figure 9.12, while the probability of failure for longitudinal steel reinforcement is shown in Figure 9.13.

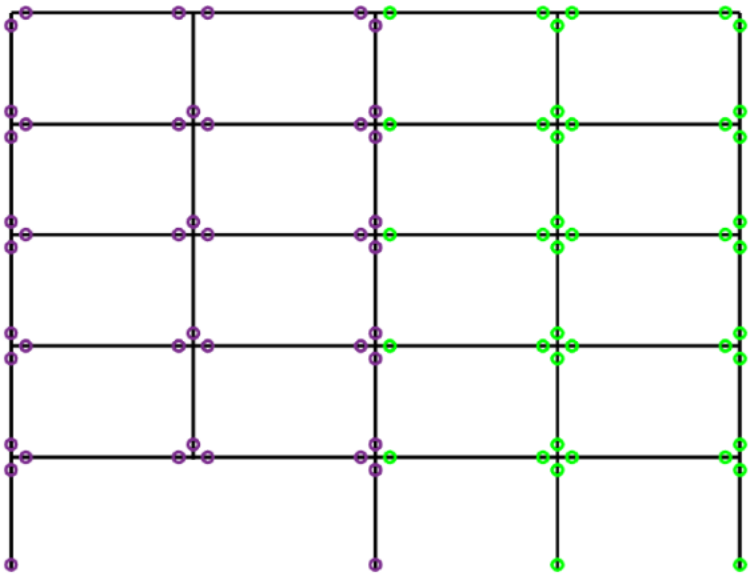

Figure 9.12 *Failure probability for concrete in frame 3*

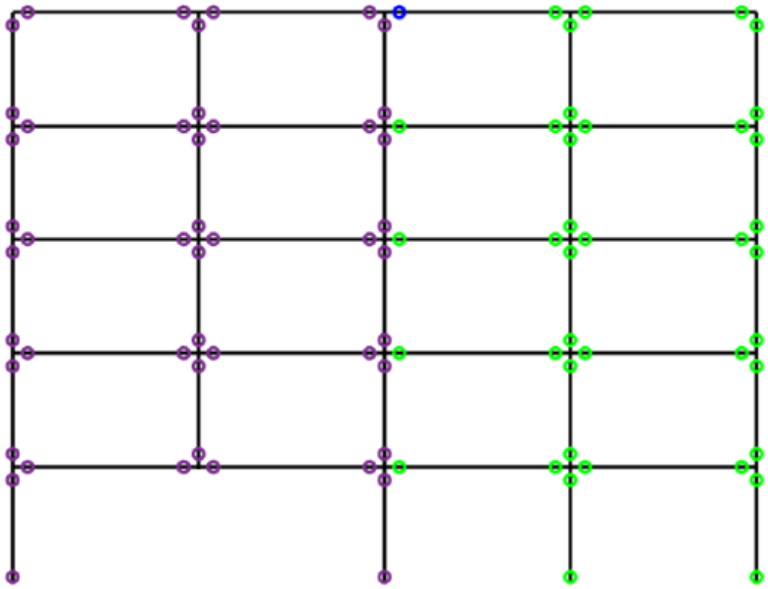

Figure 9.13 *Failure probability for steel reinforcement in frame 3*

The graphical results do not show a probability of failure for the confined concrete at the base of the nodes of the columns above the removed column for frame 2 and 3, this can be interpreted as a change in this part of the node behavior, starting to work in tension.

It is clear how the first structure, designed with standard codes, cannot support the loss of a supporting column, the probability of failure in the frame is very high, represented by the red points near the nodes for both confined concrete and longitudinal steel reinforcement. As improvements are added, such as continuity and side face rebar strategies, the probability of failure decreases slightly, finding a yellow point in the confined concrete and steel reinforcement around the area of the removed column, while the probability of failure in the half building is lower, represented by the green point.

Finally, frame 3, where all the improvements are applied, continuity, global floor equality and side face shows an intermediate level of probability failure, this is indicated by the purple points at the nodes of the frame representation, showing a clear improvement compared with the failure probability of frame 1. The two last frames show a pattern in which the area influenced by the removed column presents an intermediate level of probability of failure, while the second part of the structures have a green point for confined concrete and for longitudinal reinforcement.

Conclusions

This thesis evaluates the structural robustness of the buildings by analyzing three different structures with similar geometry but with design modifications. These design changes are applied according to strategies proposed in current codes and new proposal strategies introduced by Miceli and Castaldo (2024). The evaluated scenario of failure considers a five-story building with four spans, which is regular in both elevation and plan, and has undergone the sudden loss of the second-to-last column.

The assessment of the failure scenario follows the five-step procedure suggested by Miceli et al. (2025). In this process, five material properties and six actions suffer aleatory variations using the Latin hypercube sampled method, which generates 100 random parameters and allows 100 aleatory structures for each model. The structural capacity is analyzed throughout a nonlinear pushdown analysis using a FEM software ATENA 2D v5, the capacity curves obtained for each frame shows that frame 1, without improvements, exhibits a softening behavior with the lower peak load. As improvements are applied, the maximum peak load for the flexural stage of each frame is greater. Furthermore, it is observed how the capacity curves can present catenary behavior, where after reaching the peak load, the structure continues to deform, and in the end, the ultimate load is even higher than the peak load.

To continue the assessment of the structural scenario, a dynamic amplification factor is determined. However, this dynamic amplification factor is found only in 6% of the

iteration for frame 1, where it can be stated that external work is usually greater than internal energy. As a result, few intersections between external work and internal energy can be found, which could indicate a collapse in majority of the iterations. On the other hand, after applying some improvements, the dynamic amplification factor can be computed, and it is found in 47% of the iteration for frame 2, while for frame 3, it is not found in only 4 % of the cases.

Before determining the failure probability, a nonlinear equivalent static analysis is performed. In this analysis, external gravity loads are applied to all the spans, while only in the influence area of the removed column are the loads multiplied by the dynamic amplification factor. This approach allows the determination of the structural demand by examining the principal total strain at the nodes for the longitudinal steel reinforcement and for the confined concrete, considering only in compression, because the concrete in tension does not demonstrate a resisting behavior.

The result for the failure probability of the scenario in the three frames evaluated indicates that only the area influenced by the removed column supports the absence of the column. This means that part of the structure has a low contribution in the redistribution of the additional loads caused by the missing support, as represented by the low probability of failure in half of the structure. Meanwhile, the area directly affected by the lack of the column shows an intermediate level of failure probability, even after applying the improvement strategies, which demonstrate a significant enhancement in the structural behavior. In summary, the maximum probability of failure for the complete frame is 0.99 for frame 1, 0.57 for frame 2 and only 0.04 for frame 3.

Comparing the results with other studies, such as Miceli et al. (2025), where a similar analysis is carried out for different failure scenarios involving the removal of the central column, a clearer reduction in the probability of failure is observed after applying improvement strategies. This suggests that the loss of the second-to-last column represents a more critical case, as fewer surrounding spans are available to help redistribute the loads.

References

Adam JM, Parisi F, Sagaseta J, Lu X. “Research and practice on progressive collapse and robustness of building structures in the 21st century”. *Engineering Structures 173:122-49*, 2018.

Agarwal J, England J. “Recent developments in robustness and relation with risk”. *Proceedings of the Institution of Civil Engineers: Structures and Buildings 161(4):183-188*, 2008.

Baker JW, Schubert M, Faber MH. “On the assessment of robustness”. *Structural Safety 30(3):253–67*, 2008.

Cervenka Consulting s.r.o. “ATENA theory”. Prague, Czech Republic, 2021.

Comité Européen de Normalisation CEN. “Eurocode 1 – Actions on Structures Part 1-7: General actions - Accidental actions”. Brussels, Belgium, 2006.

Comité Européen de Normalisation CEN. “Eurocode 8 – Design of Structures for earthquake resistance”. Brussels, Belgium, 1998.

Comité Européen de Normalisation. “EN1990:2002: Eurocode 0 - basis of structural design”. Brussels, Belgium, 2002.

Ente Italiano di Normazione, “*UNI EN 206-1:2006: Calcestruzzo - Parte 1: Specificazione, prestazione, produzione e conformità*”, 2006.

Fallon, C. T., Quiel, S. E., & Naito, C. J. “Uniform pushdown approach for quantifying Building-Frame robustness and the consequence of disproportionate collapse.” *Journal of Performance of Constructed Facilities, 30(6)*, 2016.

Fascetti A, Kunnath SK, Nisticò N. “Robustness evaluation of RC frame buildings to progressive collapse”. *Engineering Structures 86:242-249*, 2015.

General Services Administration (GSA). “Progressive collapse analysis and design guidelines”. Washington, DC: Office of Chief Architects, 2003.

Haldar A, Mahadevan S. “Probability, Reliability and Statistical Methods in Engineering Design”. John Wiley, 77(5), May 2000.

International Standard Organization (ISO). “ISO 2394 General principles on reliability for structures”. 2013.

Izzuddin BA, Vlassis AG, Elghazouli AY, Nethercot DA. “Progressive collapse of multi-storey buildings due to sudden column loss - Part I: Simplified assessment framework”. *Engineering Structures* 30(5):1308–1318, 2008.

Jalayer F, Cornell CA. “Alternative Non-Linear Demand Estimation Methods for Probability-Based Seismic Assessments”. Earthquake engineering and structural dynamics 38(8):951–972, 2009

Khandelwal KS, El-Tawil S. “Pushdown resistance as a measure of robustness in progressive collapse analysis*”. Engineering Structures; 33(9):2653–61*, 2011.

Mckey MD, Conover WJ, Beckman RJ. “A comparison of three methods for selecting values of input variables in the analysis from a computer code”. *Technometrics* 21:239-45, 1979.

Miceli E, “Advances in structural robustness of reinforced concrete moment resisting frames”. Doctoral thesis. Turin: Politecnico di Torino, 2024.

Miceli E, Castaldo P. “Robustness Improvements for 2D Reinforced Concrete Moment Resisting Frames: Parametric Study by Means of NLFE Analyses”. *Structural concrete: journal of the fib Structural Concrete 25(1):9-31*, 2024.

Miceli E, Gino D, Castaldo P. “Approaches to estimate global safety factors for reliability assessment of RC structures using non-linear numerical analyses”. *Engineering Structures*, 2024.

Miceli, E., Gino, D., Castaldo, P., “RELIABILITY ASSESSMENT OF ROBUSTNESS FOR REINFORCED CONCRETE MOMENT RESISTING FRAMES”, *Developments in the Built Environment*, https://doi.org/10.1016/j.dibe.2025.100639.

Ministero delle Infrastrutture e dei Trasporti. Norme tecniche per le costruzioni 2018 (NTC 2018). Gazzetta Ufficiale della Repubblica Italiana, 2018.

Pearson C, Delatte N. “Ronan Point Apartment Tower Collapse and its Effect on Building Codes”. *Journal of Performance of Constructed Facilities, 19(2), 172–177*, 2005.

Ślaga L. “Catenary action in precast skeleton structures -protection against progressive collapse” *Conference: 15th International Conference of Postgraduate Students JUNIORSTAV*, 2013.

Starossek U, Haberland M. “Approaches to measures of structural robustness”. *Structure and Infrastructure Engineering 7:625-631*, 2011.

Zheng T, Zhong W, Bao M., Zheng Y, Duan S. “Effect of various boundary constraints on the collapse behavior of multi-story composite frames”. *Journal of Building Engineering 52:104412*, 2022.